A Novel Skeleton-Based Human Activity Discovery Using Particle Swarm Optimization with Gaussian Mutation

Parham Hadikhani*, Daphne Teck Ching Lai and Wee-Hong Ong

The proposed method is presented, as shown in Fig. 1.

The process of Keyframe selection is shown in Fig. 2.

The geometric illustration of how to decode the PSO particles to obtain a set of clusters and the Evolution of particles is shown in Fig. 3. The routine of the proposed clustering algorithm is shown in Algorithm 1.

Algorithm 1: Hybrid PSO with Gaussian Mutation and K-means (HPGMK)

Input: D=$\{d_1,d_2,\ldots,d_n\}$ //Set of data points
k //Number of desired activities (clusters)
Output: Set of k clusters

Initialize a population of particles with random positions and velocities in the search space
for *t=1 to the maximum number of iteration* **do**
  for *each particle i* **do**
    Update position and velocity of particle i according to Eq.(10) and Eq.(11) in the main manuscript
    Evaluate fitness value of particle i according to the fitness function in Eq.(15) in the main manuscript
    Update $pbest_i$(t) and *gbest*(t) if necessary
    for *T times (T is the number of iteration for mutation and set 10)* **do**
      Mutate *gbest*(t) according to Eq.(16) and (17) in the main manuscript
      Compare mutated *gbest*(t) with previous and choose the best as new *gbest*(t)
Use *gbest*(t) as the initial centroids
while *until no change* **do**
  `// Refining the centroids`
  Calculate distances of data points to centroids
  Assign data points to the closest cluster
  Centroids are updated using the following equation $centroid_i = \frac{1}{n_i}\sum_{\forall d_i \in C_i} d_i$,
  where n_i is the number of data points in the cluster i

P. Hadikhani, D.T.C. Lai, and W.H. Ong are with the School of Digital Science, Universiti Brunei Darussalam, Brunei. E-mail: {20h8561, daphne.lai, weehong.ong}@ubd.edu.bn.

I. Experiments

A. Datasets

Five datasets were used to evaluate the effectiveness of proposed method: Cornell Activity Dataset (CAD-60) [1], UTKinect-Action3D (UTK) [2], Florence3D (F3D) [3], Kinect Activity Recognition Dataset (KARD) [4], and MSR DailyActivity3D (MSR) [5]. These datasets have different dimensions, features, and activities. Table I shows the statistical information of these datasets. They are discussed as follows.

TABLE I: Number of activities, subjects and videos in the five datasets used

Dataset	CAD-60	UTK	F3D	KARD	MSR
Activities	14	10	9	18	16
Subjects	4	10	10	10	10
Videos	60	200	215	2160	320

CAD-60: This dataset includes 14 activities: *rinsing mouth*, *brushing teeth*, *wearing contact lens*, *talking on the phone*, *drinking water*, *opening pill container*, *cooking (chopping)*, *cooking (stirring)*, *talking on couch*, *relaxing on couch*, *writing on whiteboard*, *still (standing)*, *working on computer* and *random*. Each activity was performed by 4 subjects including one left-handed person. They were performed in 5 different environments: bathroom, bedroom, kitchen, living room, and office. It contains activities of cyclic nature such as *brushing teeth* and activities with similar postures such as *drinking water* and *talking on the phone*.

UTK: There are 10 activities in this dataset: *walk*, *sit down*, *stand up*, *pick up*, *carry*, *throw*, *push*, *pull*, *wave hands*, and *clap hands*. These activities were performed by 10 subjects and repeated twice by each subject. The significant intra-class and viewpoint variations are the main challenges of this dataset.

F3D: This dataset includes 9 activities: *wave*, *drink from a bottle*, *answer phone*, *clap*, *tight lace*, *sit down*, *stand up*, *read watch*, and *bow*. These activities were repeated twice or thrice by 10 subjects. The main challenge with this dataset is that the activities were performed at high speed. This provides a small number of frames for the algorithm to sample and learn from.

KARD: This dataset contains 2160 videos and consists of 18 activities. These activities were performed by 10 different people. The 18 activities are *horizontal arm wave*, *high arm wave*, *two hand wave*, *catch cap*, *high throw*, *draw X*, *draw*

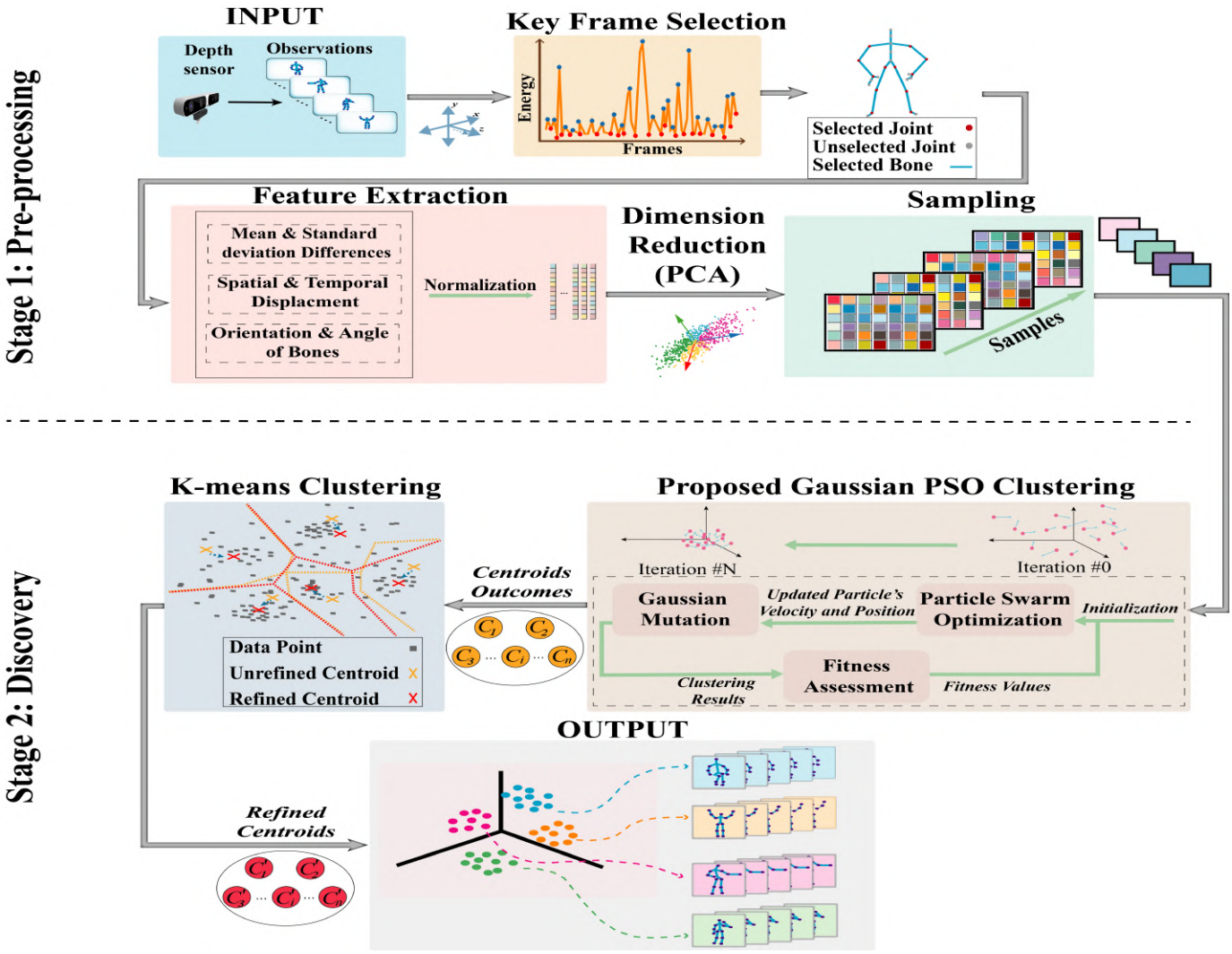

Fig. 1: Methodology of the proposed approach has two stage pre-processing and discovery. In pre-processing, keyframes are selected from the video sequence by computing kinetic energy. Then, features based on different aspects of skeleton including displacement, orientation, and statistical are extracted from informative joints and bones. Principal components are then chosen by applying PCA on the features. Next, overlapping time windows is used to segment a series of keyframes as activity samples. In discovery stage (HPGMK), Hybrid PSO clustering with Gaussian mutation operator is used to discover the groups of activities. Eventually, K-means clustering is applied to the resultant cluster centers to refine the centroids.

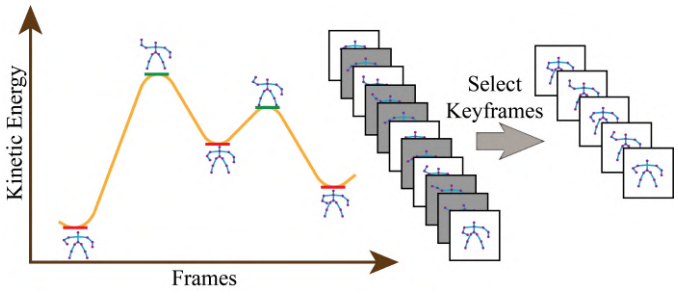

Fig. 2: Illustration of the keyframe selection.

tick, *toss paper*, *forward kick*, *side kick*, *take umbrella*, *bend*, *hand clap*, *walk*, *phone call*, *drink*, *sit down*, and *stand up*. This dataset is challenging due to the large number of activities with high intra-class variation such as different individuals performing the same activity such as catch cap but in different ways, this makes learning of the same activity with large differences in movements difficult.

MSR: In this dataset there are 16 activities: *drink*, *eat*, *read book*, *call cellphone*, *write on a paper*, *use laptop*, *use vacuum cleaner*, *cheer up*, *sit still*, *toss paper*, *play game*, *lie down on sofa*, *walk*, *play guitar*, *stand up*, and *sit down*. There are 10 subjects, and each subject performed all activities in both standing and sitting positions. This makes the dataset challenging because the extracted features for both sitting and standing positions in each activity are different. Another challenge is data corruption. In some frames, the skeletal gesture structure suddenly collapses completely and lose their coherence and become meaningless.

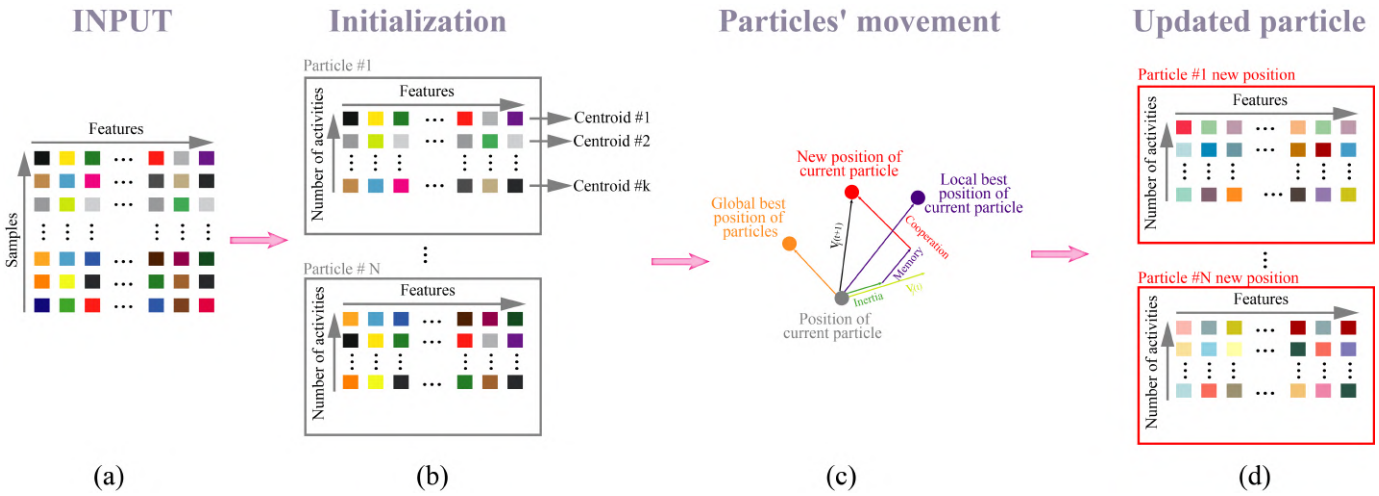

Fig. 3: Illustration of decoding the solution of PSO to get a set of clusters. (a) Samples with extracted features are given as input to PSO algorithm. (b) Then, each particle randomly chooses as many as the number of activities (clusters) from samples and (c) based on the PSO operation (d) updates its position.

B. Parameters setting

Through preliminary experiments, the best values for swarm size and the number of iterations were 20 and 50, respectively. The experiment was repeated 30 times and the average was obtained. The parameter settings of the HPGMK is summarized in Table II.

TABLE II: Parameters setting used in the experiment.

Parameter	Description	Value
$c1_{max}, c2_{max}$	acceleration coefficients	2.5
$c1_{min}, c2_{min}$	acceleration coefficients	0
w_{max}	inertial weight	0.9
t	maximum number of iteration	50
T	number of iteration for mutation	10
np	swarm size	20

C. Computation complexity analysis

The Computation complexity of HPGMK in the initial stage (step 1 in Algorithm 1) is equal to $O(D.k.dim.np)$, where D is the number of data points, k is the number of clusters, dim is the dimension of data points and np is the population size of particles. The time complexity when particles are updated (step 2 to 9) is equal to $O(t.dim.T.np)$, where t is maximum number of iteration and T is the number of iteration for mutating *gbest*(t). In Refining obtained centroids (step 11 to 15), the time complexity is equal to $O(log(D.k.dim))$. Therefore, the overall computation complexity of proposed algorithm is equal to $O(t.T.np.D.k.dim + log(D.k.dim))$. Table III shows the comparison of the computation complexity of the well-known clustering algorithms including KM and BIRCH along with the state-of-the-art algorithms developed for clustering with the proposed algorithm. Based on the results, PSO-based clustering algorithms take substantially longer to execute than non-PSO-based clustering methods. But despite the low time complexity of KM and BIRCH clustering, their accuracy is very low and they need to be executed many times to reach the desired solution if they do not get stuck in the local optimum. HPSOK-means, MinMaxK-means, PSC-RCE, PSOLFK and PSOSCALFK have around the same time complexity. However, we developed an algorithm, which has powerful global search capabilities due to increasing the variety of solutions during the execution of the algorithm by applying Guassina mutation and modifying the cluster using KM to increase the ability of PSO in local search.

TABLE III: The computation complexity of HPGMK and eight related algorithms.

Algorithm	Computation Complexity
KM	$O(N.K.D.t)$
BIRCH	$O(N)$
HPSOK-means	$O(N.K.D.t)$
MinMaxK-means	$O(N.K.D.t)$
PSC-RCE	$O(N.K.D.n_m.t)$
PSOLFK	$O(N.K.D.t)$
PSOSCALFK	$O(N.K.D.t)$
KMM	$O((N.dim + m^2 + m.k).t + m.dim)$
GLPSOK	$O(K.dim.(K.dim + N).t)$
HPGMK	$O(t.T.np.D.k.dim + log(D.k.dim))$

To show activity discovery performance, we show the confusion matrix in Fig. 4 to 8 for different methods applied on five datasets used in this paper. These figures demonstrate that HPGMK produced distinctively meaningful clusters. In these figures, cluster overlapping appears relatively high in the other methods especially KM and SC in all datasets. In CAD-60 (Fig. 4), the worst confusion occured between *brushing teeth* and *random* due to similar body gestures. There was also activity overlapping between *brushing teeth*, and *wearing contact lenses*, because of similar hand movement near the head. In UTK (Fig. 5), the following activity pairs were poorly

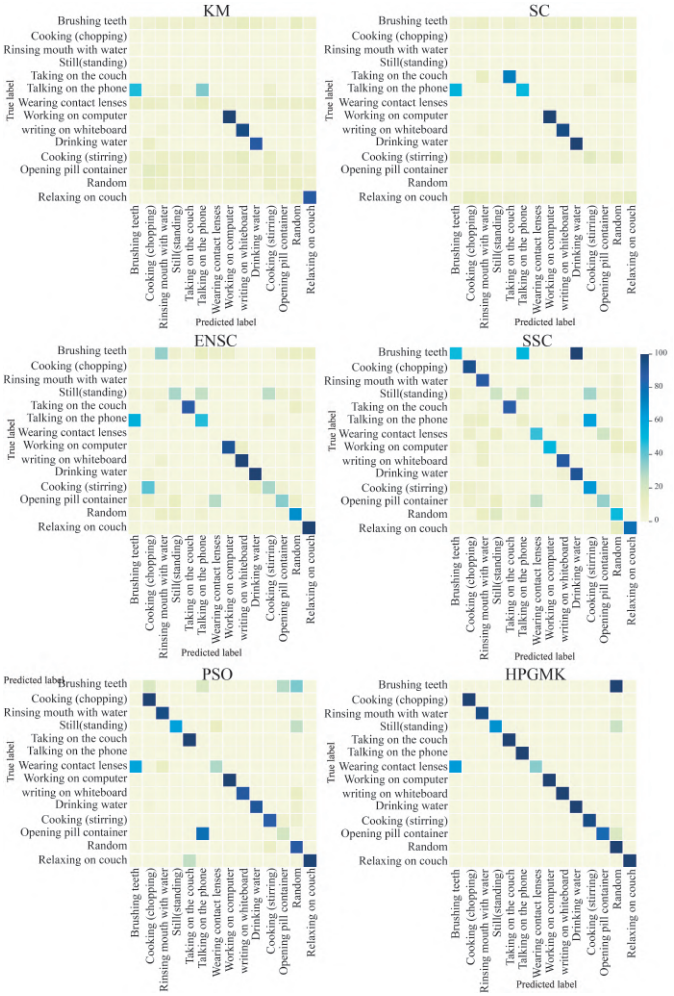

Fig. 4: Comparison of confusion matrix of the result on subject 1 in CAD-60. Activity list: (1) Brushing teeth; (2) Cooking (chopping); (3) Rinsing mouth with water; (4) Still(standing); (5) Taking on the couch; (6) Talking on the phone; (7) Wearing contact lenses; (8) Working on computer; (9) Writing on whiteboard; (10) Drinking water; (11) Cooking (stirring); (12) Opening pill container; (13) Random; and (14) Relaxing on couch.

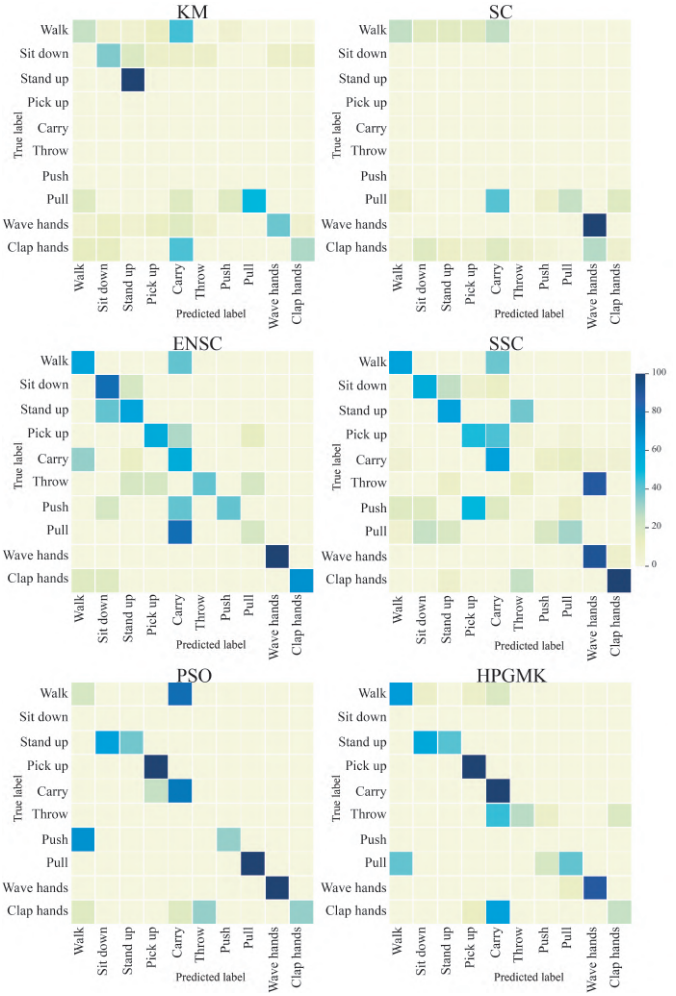

Fig. 5: Comparison of confusion matrix of the result on subject 8 in UTK. Activity list: (1) Walk; (2) Sit down; (3) Stand up; (4) Pick up; (5) Carry; (6) Throw; (7) Push; (8) Pull; (9) Wave hands; and (10) Clap hands.

distinguished between each other, *sit down* with *stand up* and *push* with *pull*. These two similar activities are performed inversely with each other, so they are difficult to distinguish. In datasets KARD (Fig. 7) and MSR (Fig. 8), there were a lot of overlapping due to the large number of activities that are very similar. For instance, in Fig. 7, activity overlapping were seen between *draw x* and *draw tick*, *forward kick* and *side kick*, *two hand wave* and *hand clap*, *catch cap* and *take umbrella*, *horizontal arm wave* and *hand clap*, and *bend* and *drink*.

Fig. 9 to 13 show the average F-score for each activity for all subjects. By examining the average F-scores in all datasets , it shows HPGMK outperforming other methods in all datasets used. HPGMK achieved slightly under 75 % on CAD-60, just over 45 % on UTK, almost 60 % on F3D, around 40 % on KARD, and almost 30 % on MSR . In Fig. 9, for HPGMK although F-score was high in most of the activities compared to other methods, *cooking (chopping)* and *talking on the phone* were discovered with low F-scores. This was due to the high similarity between *cooking (chopping)* with *cooking (stirring)* and *talking on the phone* with *wearing contact lenses*. In Fig. 10, a few actions were discovered with low F-scores. For example, *throw* samples were easily mistakenly regarded as *push* due to similar hand movements, resulting in low F-scores in both activities. In Fig. 11, we observe HPGMK outperformed other methods except for activities *wave*, *clap* and *tight lace*. With respect to the F-score of KARD dataset in Fig. 12, activities such as *horizontal arm wave*, *high arm wave*, *high throw*, *phone call*, and *drink* have achieved lower F-score than the other activities due to the large number of similar activities that were performed by hand. In Fig. 13, the F-score for most of the activities were below 40 %. The reason for the low value of F-score for activities in MSR is the presence of a lot of noise in the data and also activities were performed in both standing and sitting. Fig. 14 shows the average clustering time of the different combinations of

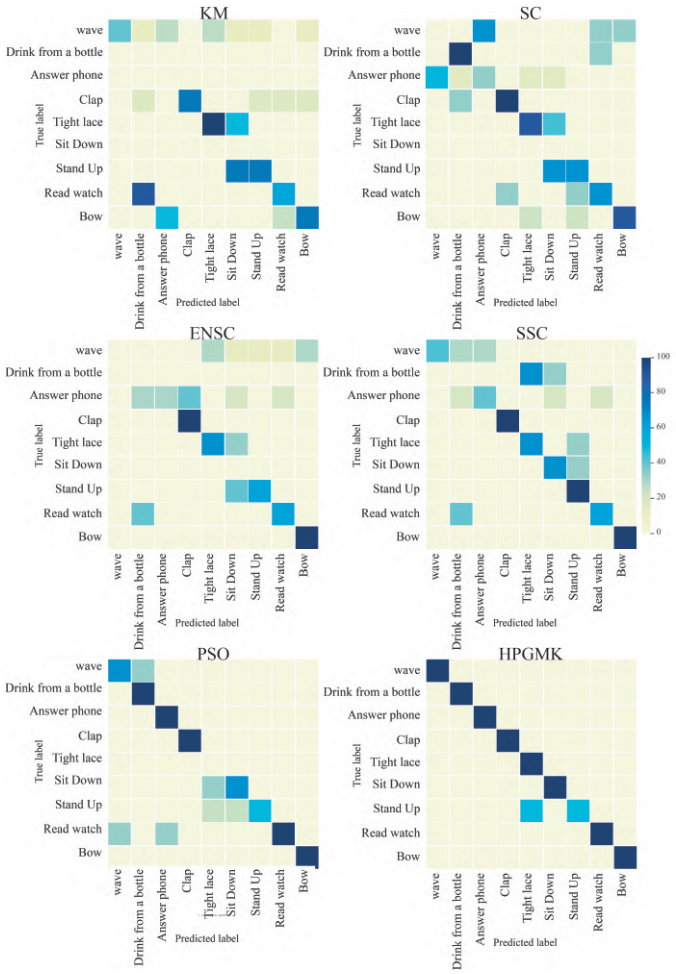

Fig. 6: Comparison of confusion matrix of the result on subject 2 in F3D. Activity list: (1) Wave; (2) Drink from a bottle; (3) Answer phone; (4) Clap; (5) Tight lace; (6) Sit down; (7) Stand up; (8) Read watch; and (9) Bow.

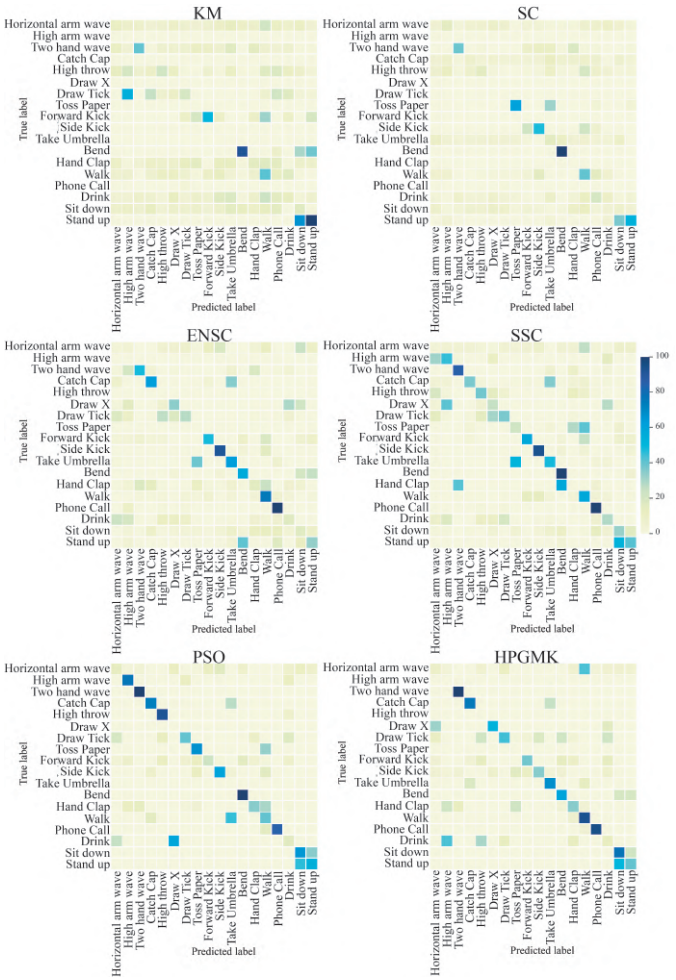

Fig. 7: Comparison of confusion matrix of the result on subject 10 in KARD. Activity list: (1) Horizontal arm wave; (2) High arm wave; (3) Two hand wave; (4) Catch cap; (5) High throw; (6) Draw X; (7) Draw tick; (8) Toss paper; (9) Forward kick; (10) side kick; (11) Take umbrella; (12) Bend; (13) Hand clap; (14) Walk; (15) Phone call; (16) Drink; (17) Sit down; and (18) Stand up.

components used in the proposed algorithm in milliseconds on subject 1 in CAD-60. This experiment evaluates the impact of the different components in the proposed HPGMK algorithm. As can be seen, the clustering time of the proposed algorithm (red line) was relatively low. The reason is that our approach has benefited from dimension reduction methods, including PCA and keyframe selector. Fig. 15 indicates the effect of each component of HPGMK on convergence rate. As it is indicated, each combination has a different convergence rate. However, using all components enables the proposed method to achieve the best convergence compared to the other combinations. It is also confirmed from Fig. 15 that by combining both KM and PSO algorithms, the convergence speed has increased. Table IV indicates a significant difference between the HPGMK and KM, HPGMK and PSO, HPGMK and SSC, HPGMK and ENSC and HPGMK and SDCN through 30 independent runs using the Kruskal–Wallis test (p-value). Since the p-value of almost all of the datasets is less than 0.05 (significance level) with the 95 % confidence intervals for each median, we reject the null hypothesis, and conclude there is a significant difference between the proposed method with KM, PSO, SSC, ENSC, and SDCN. In cases where the p-value is higher than the significant level (these cases are specified with* in Table IV), there is not enough evidence to reject the null hypothesis.

TABLE IV: Comparison of Kruskal-Wallis test (p-value) between HPGMK and KM, HPGMK and PSO, HPGMK and SSC, HPGMK and ENSC and HPGMK and SDCN through 30 independent runs

Datasets	HPGMK vs KM	HPGMK vs PSO	HPGMK vs SDCN	HPGMK vs ENSC	HPGMK vs SSC
CAD-60	≈0	0.00048	≈0	≈0	
UTK	≈0	0.00014	0.02369*	≈0	0.03325*
F3D	≈0	≈0	≈0	≈0	≈0
KARD	≈0	0.00544	0.023696*	≈0	0.39117*
MSR	≈0	0.88246*	≈0	≈0	0.018736*

* p-value $>$ 0.05: The differences between the medians are not statistically significant.

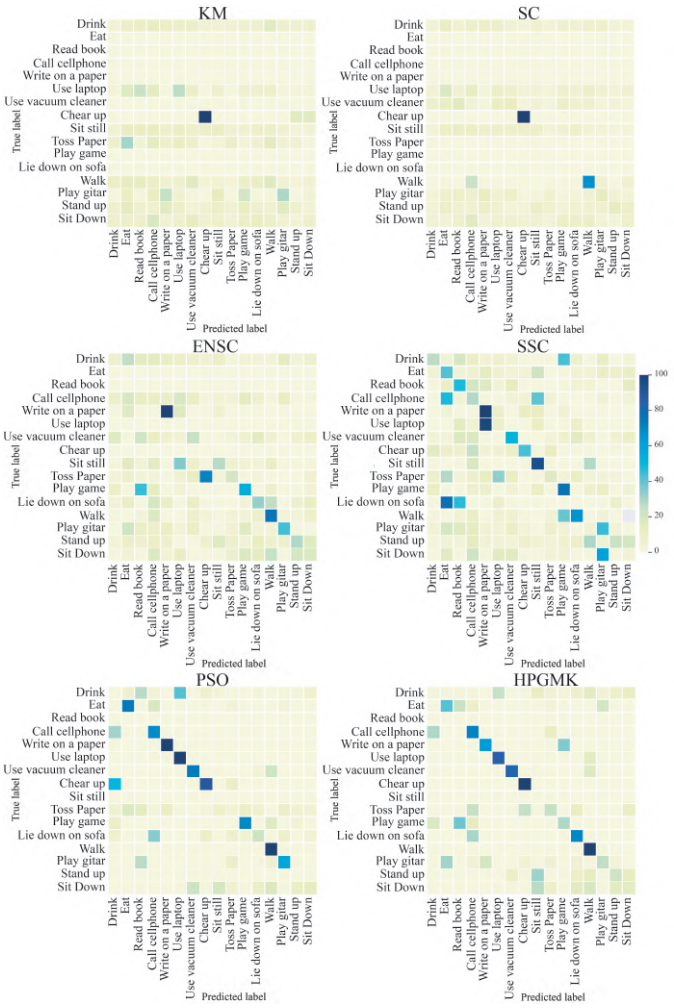

Fig. 8: Comparison of confusion matrix of the result on subject 5 in MSR. Activity list: (1) Drink; (2) Eat; (3) Read book; (4) Call cellphone; (5) Write on a paper; (6) Use laptop; (7) Use vacuum cleaner; (8) Cheer up; (9) Sit still; (10) Toss paper; (11) Play game; (12) Lie down on sofa; (13) Walk; (14) Play guitar; (15) Stand up; and (16) Sit down.

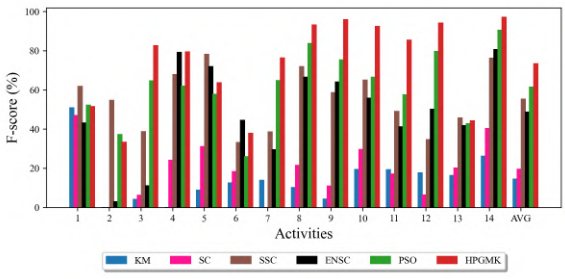

Fig. 9: The average F-score for all subjects in CAD-60. Activity list: (1) Brushing teeth; (2) Cooking (chopping); (3) Rinsing mouth with water; (4) Still(standing); (5) Taking on the couch; (6) Talking on the phone; (7) Wearing contact lenses; (8) Working on computer; (9) Writing on whiteboard; (10) Drinking water; (11) Cooking (stirring); (12) Opening pill container; (13) Random; and (14) Relaxing on couch. AVG is the average F-score for all activities.

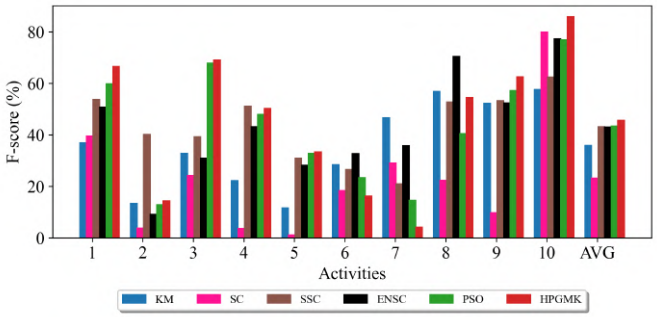

Fig. 10: The average F-score for all subjects in UTK. Activity list: (1) Walk; (2) Sit down; (3) Stand up; (4) Pick up; (5) Carry; (6) Throw; (7) Push; (8) Pull; (9) Wave hands; and (10) Clap hands. AVG is the average F-score for all activities.

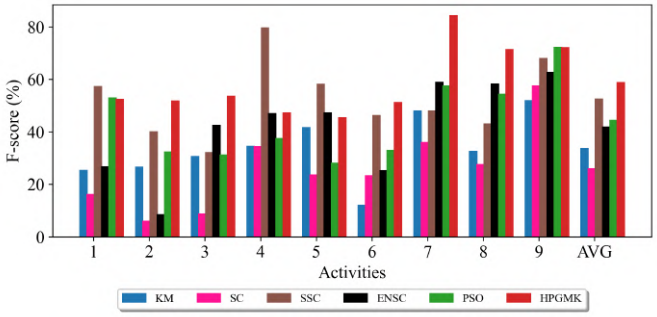

Fig. 11: The average F-score for all subjects in F3D. Activity list: (1) Wave; (2) Drink from a bottle; (3) Answer phone; (4) Clap; (5) Tight lace; (6) Sit down; (7) Stand up; (8) Read watch; and (9) Bow. AVG is the average F-score for all activities.

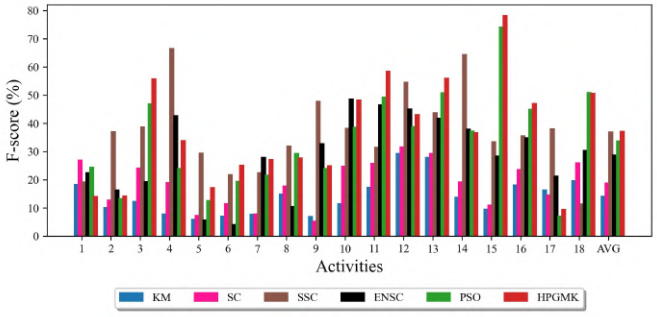

Fig. 12: The average F-score for all subjects in KARD. Activity list: (1) Horizontal arm wave; (2) High arm wave; (3) Two hand wave; (4) Catch cap; (5) High throw; (6) Draw X; (7) Draw tick; (8) Toss paper; (9) Forward kick; (10) side kick; (11) Take umbrella; (12) Bend; (13) Hand clap; (14) Walk; (15) Phone call; (16) Drink; (17) Sit down; and (18) Stand up. AVG is the average F-score for all activities.

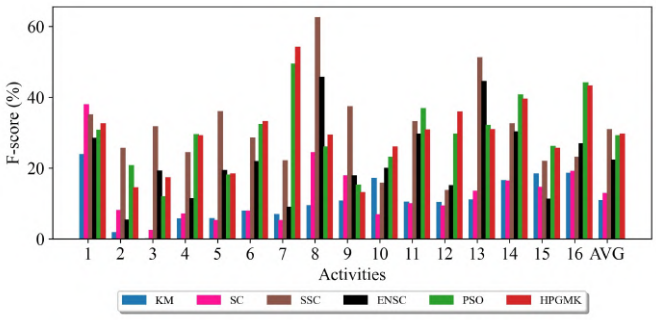

Fig. 13: The average F-score for all subjects in MSR. Activity list: (1) Drink; (2) Eat; (3) Read book; (4) Call cellphone; (5) Write on a paper; (6) Use laptop; (7) Use vacuum cleaner; (8) Cheer up; (9) Sit still; (10) Toss paper; (11) Play game; (12) Lie down on sofa; (13) Walk; (14) Play guitar; (15) Stand up; and (16) Sit down. AVG is the average F-score for all activities.

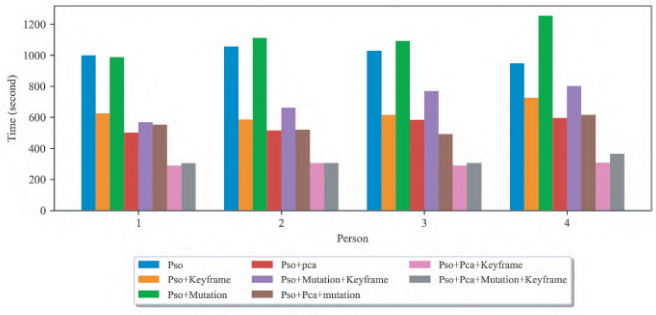

Fig. 14: The comparison of clustering time of different components of proposed algorithm on all subjects in CAD-60.

Figure 15-19 visually shows the average clustering time of the eight clustering algorithms in milliseconds on the 5 datasets. As shown, compared with the other seven algorithms, the clustering time of the proposed algorithm (gray line) is relatively low. Because our approach enjoys the benefits of dimension reduction methods including PCA and Keyframe selector. That is why it achieves a lower clustering time. Moreover, by combing both these algorithms the convergence speed is accelerated as validated in Figure 20-62.It is also confirmed that by combining both K-means and PSO algorithms, the convergence speed increases. Figure 63-107 show the confusion matrix of HPGMK for each subject in different datasets.

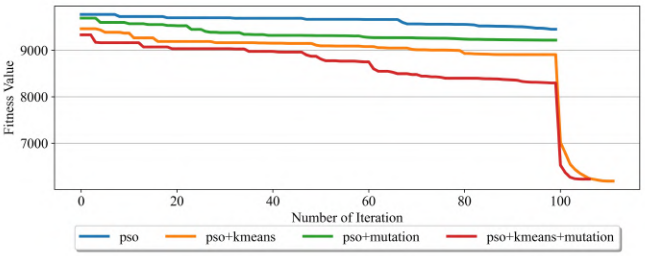

Fig. 15: The comparison of convergence in subject 1 of CAD-60.

REFERENCES

[1] J. Sung, C. Ponce, B. Selman, and A. Saxena, "Unstructured human activity detection from rgbd images," in *2012 IEEE international conference on robotics and automation*. IEEE, 2012, pp. 842–849.

[2] L. Xia, C.-C. Chen, and J. K. Aggarwal, "View invariant human action recognition using histograms of 3d joints," in *2012 IEEE computer society conference on computer vision and pattern recognition workshops*. IEEE, 2012, pp. 20–27.

[3] L. Seidenari, V. Varano, S. Berretti, A. Bimbo, and P. Pala, "Recognizing actions from depth cameras as weakly aligned multi-part bag-of-poses," in *Proceedings of the IEEE Conference on Computer Vision and Pattern Recognition Workshops*, 2013, pp. 479–485.

[4] S. Gaglio, G. L. Re, and M. Morana, "Human activity recognition process using 3-d posture data," *IEEE Transactions on Human-Machine Systems*, vol. 45, no. 5, pp. 586–597, 2014.

[5] J. Wang, Z. Liu, Y. Wu, and J. Yuan, "Mining actionlet ensemble for action recognition with depth cameras," in *2012 IEEE Conference on Computer Vision and Pattern Recognition*. IEEE, 2012, pp. 1290–1297.

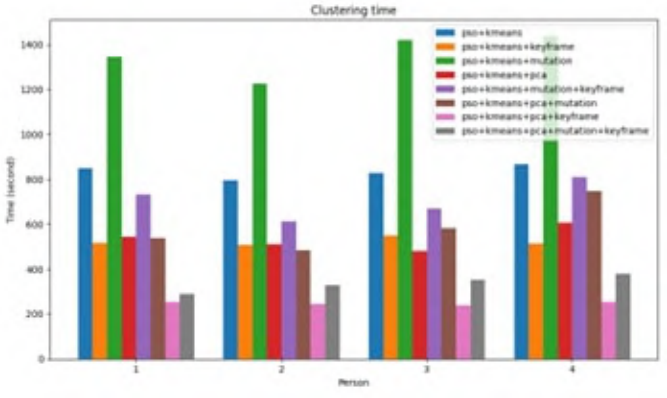

Fig. 16: The comparison of clustering time for all subjects of CAD-60.

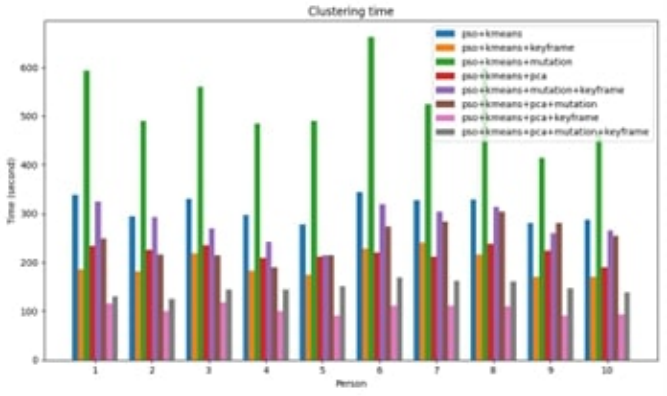

Fig. 17: The comparison of clustering time for all subjects of KARD.

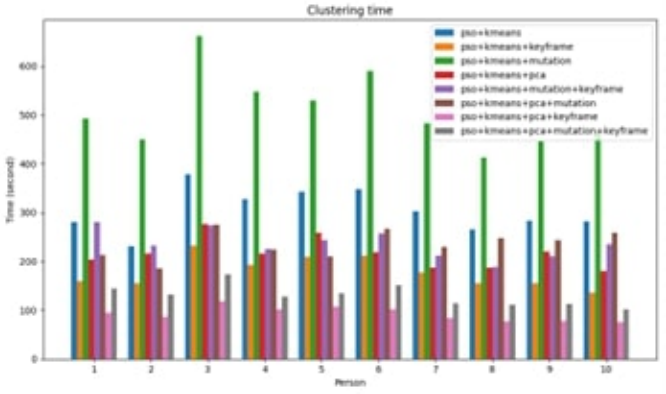

Fig. 18: The comparison of clustering time for all subjects of MSR.

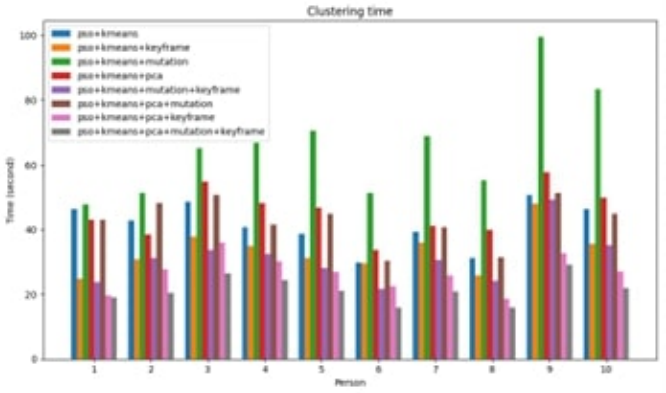

Fig. 19: The comparison of clustering time for all subjects of UTK.

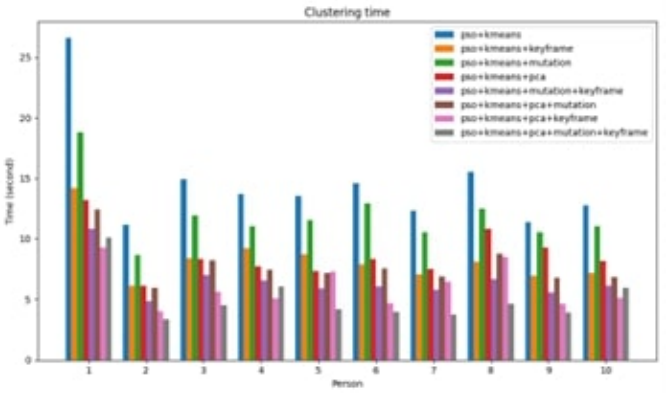

Fig. 20: The comparison of clustering time for all subjects of F3D.

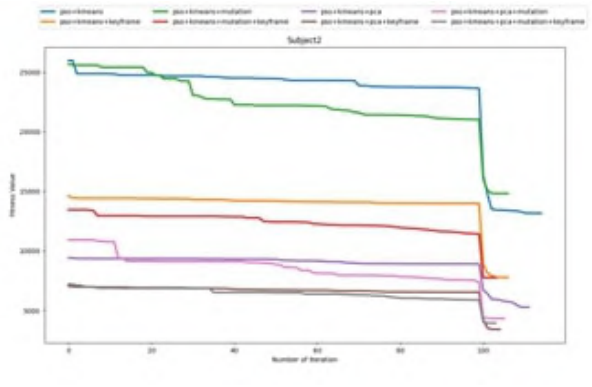

Fig. 21: The comparison of convergence in subject 1 of CAD-60.

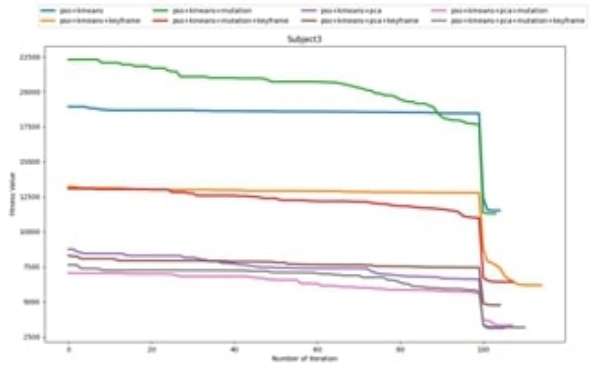

Fig. 22: The comparison of convergence in subject 2 of CAD-60.

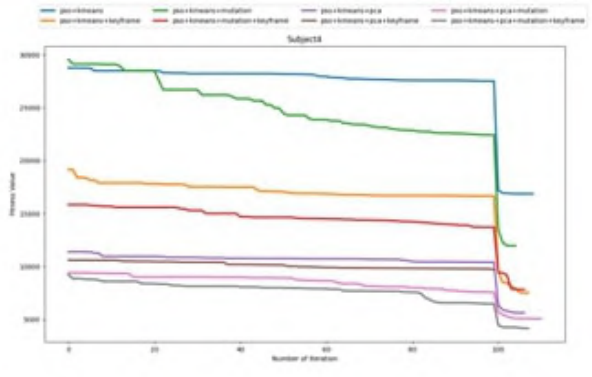

Fig. 23: The comparison of convergence in subject 3 of CAD-60.

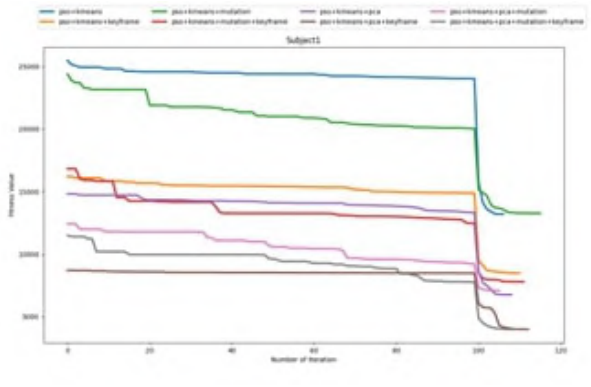

Fig. 24: The comparison of convergence in subject 4 of CAD-60.

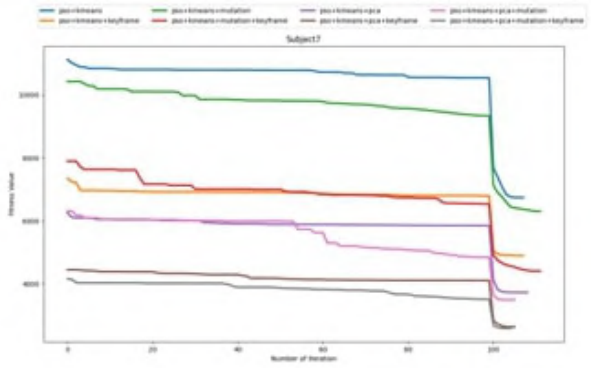

Fig. 25: The comparison of convergence in subject 1 of KARD.

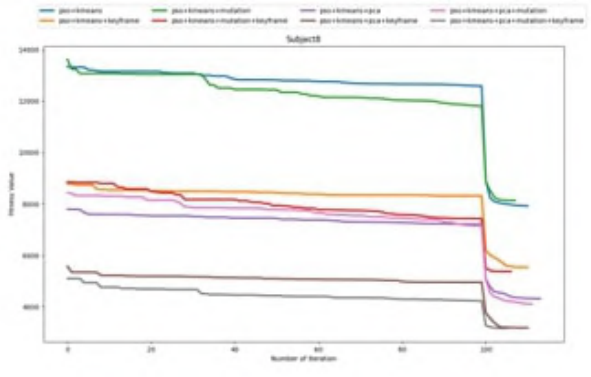

Fig. 26: The comparison of convergence in subject 2 of KARD.

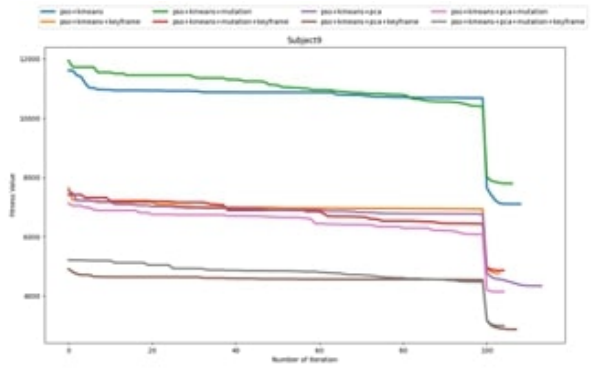

Fig. 27: The comparison of convergence in subject 3 of KARD.

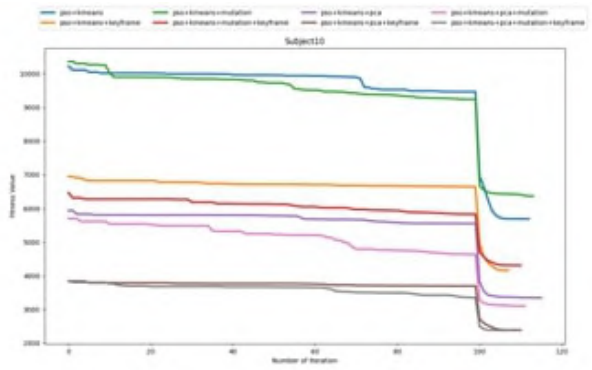

Fig. 28: The comparison of convergence in subject 4 of KARD.

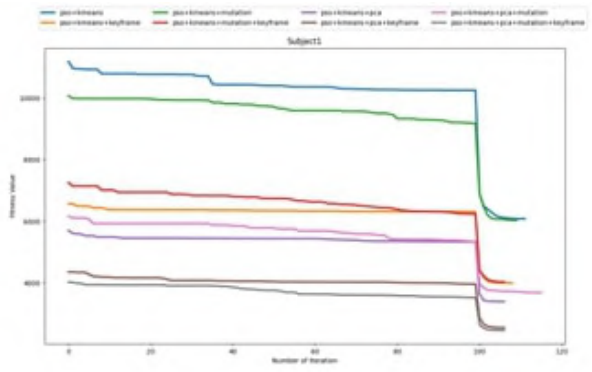

Fig. 29: The comparison of convergence in subject 5 of KARD.

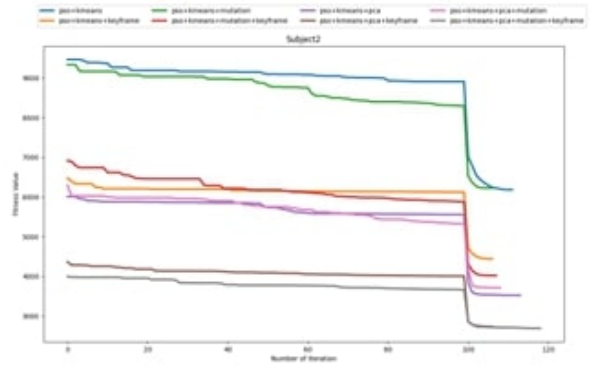

Fig. 30: The comparison of convergence in subject 6 of KARD.

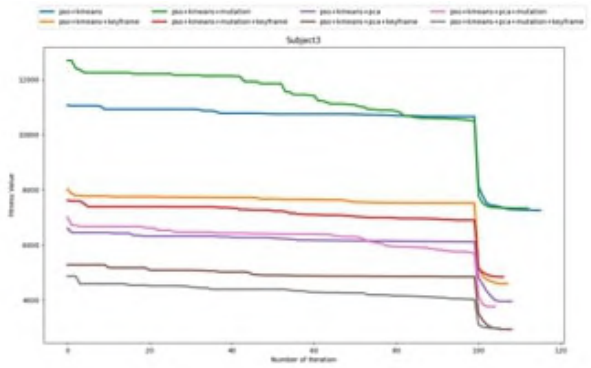

Fig. 31: The comparison of convergence in subject 7 of KARD.

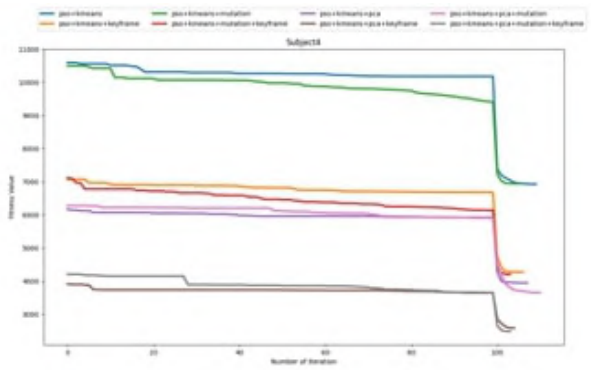

Fig. 32: he comparison of convergence in subject 8 of KARD.

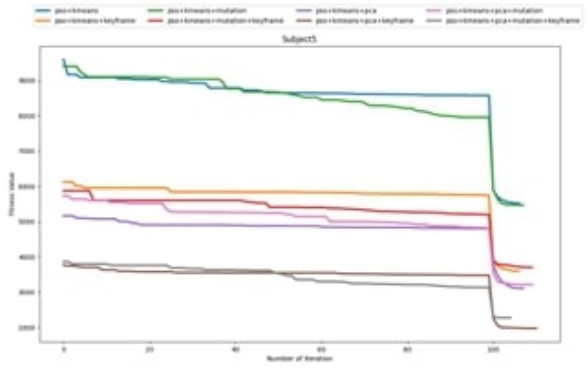

Fig. 33: The comparison of convergence in subject 9 of KARD.

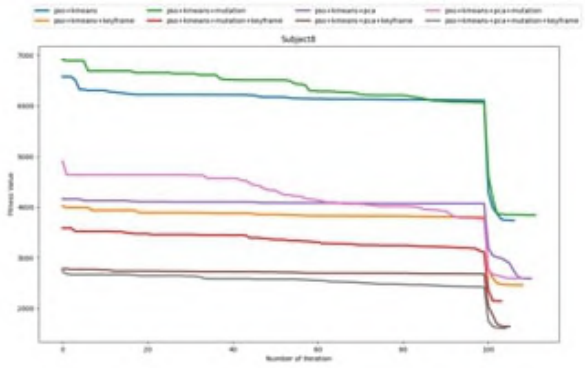

Fig. 36: The comparison of convergence in subject 2 of MSR.

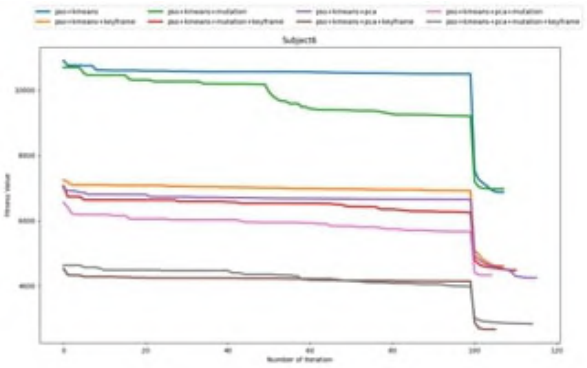

Fig. 34: The comparison of convergence in subject 10 of KARD.

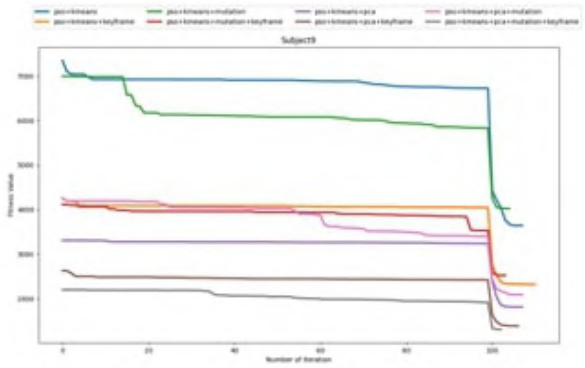

Fig. 37: The comparison of convergence in subject 3 of MSR.

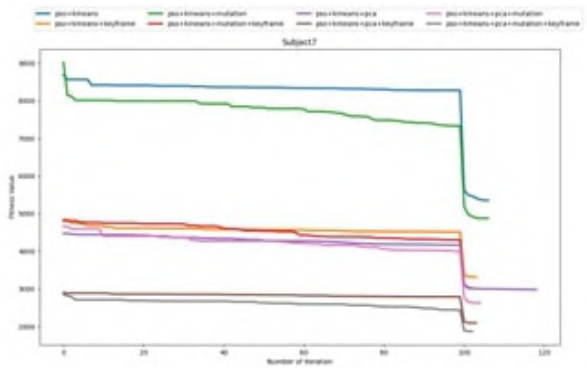

Fig. 35: The comparison of convergence in subject 1 of MSR.

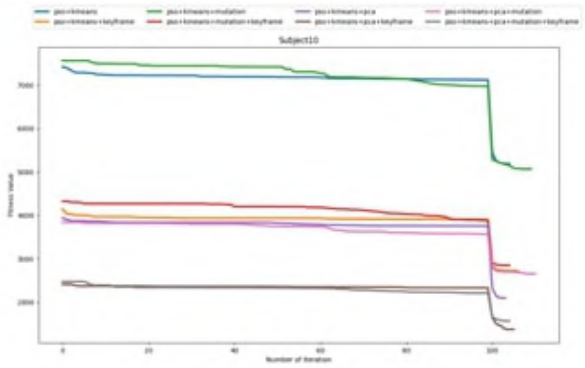

Fig. 38: The comparison of convergence in subject 4 of MSR.

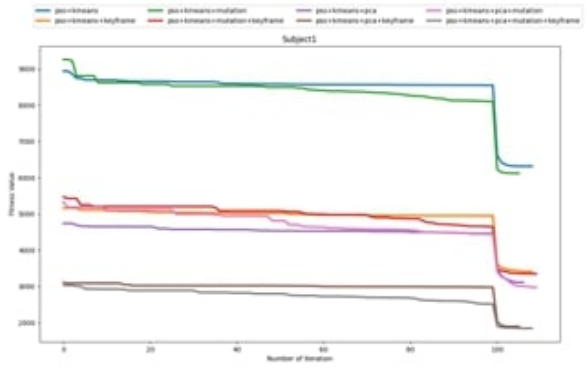

Fig. 39: The comparison of convergence in subject 5 of MSR.

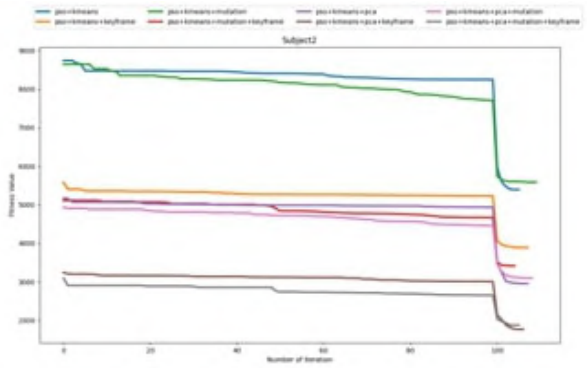

Fig. 40: The comparison of convergence in subject 6 of MSR.

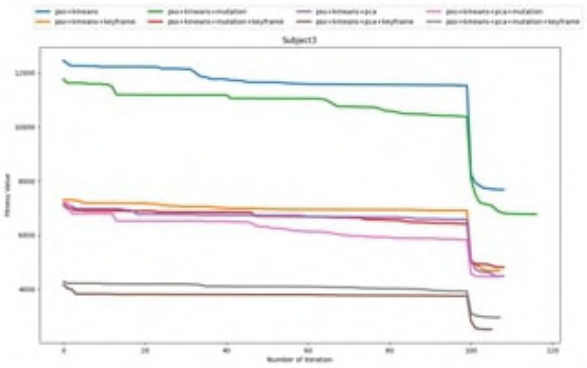

Fig. 41: The comparison of convergence in subject 7 of MSR.

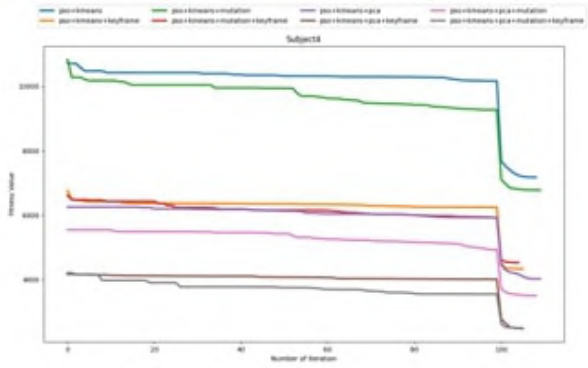

Fig. 42: The comparison of convergence in subject 8 of MSR.

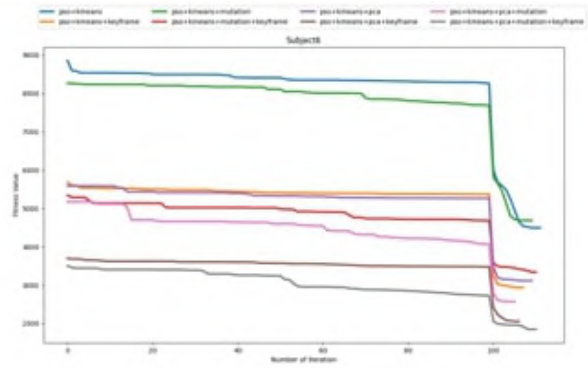

Fig. 43: The comparison of convergence in subject 9 of MSR.

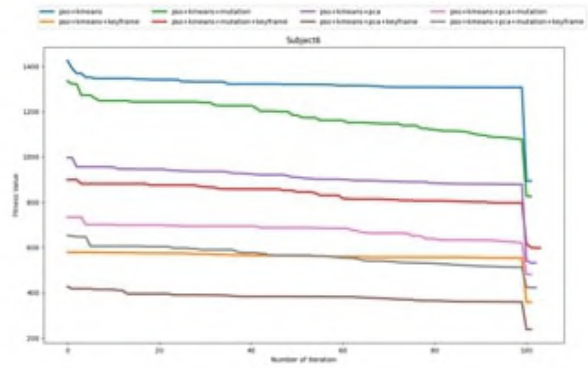

Fig. 44: The comparison of convergence in subject 10 of MSR.

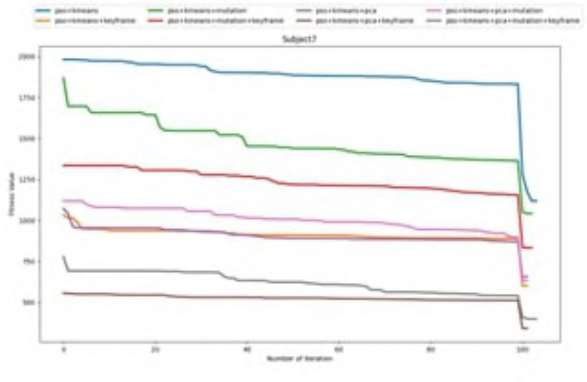

Fig. 45: The comparison of convergence in subject 1 of UTK.

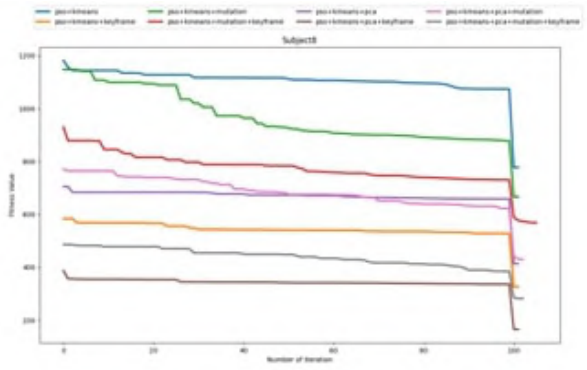

Fig. 46: The comparison of convergence in subject 2 of UTK.

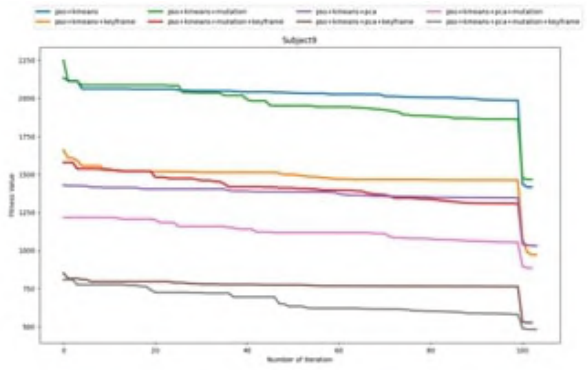

Fig. 47: The comparison of convergence in subject 3 of UTK.

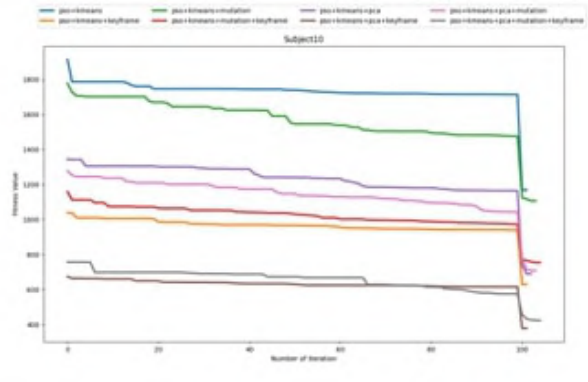

Fig. 48: The comparison of convergence in subject 4 of UTK.

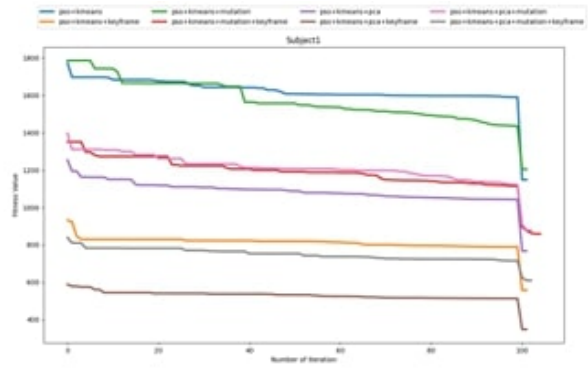

Fig. 49: The comparison of convergence in subject 5 of UTK.

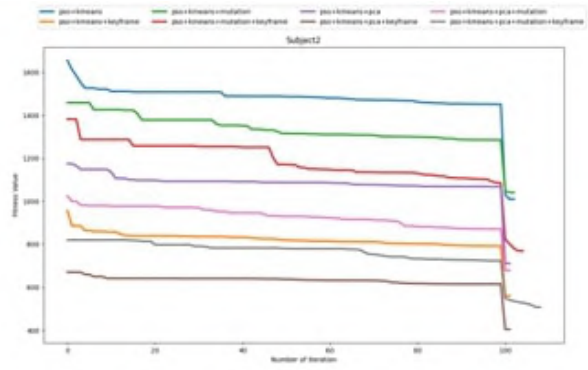

Fig. 50: The comparison of convergence in subject 6 of UTK.

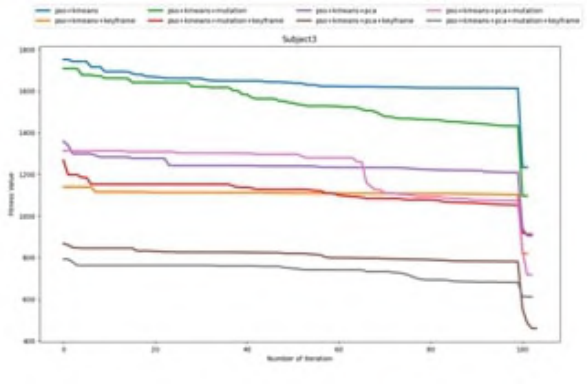

Fig. 51: The comparison of convergence in subject 7 of UTK.

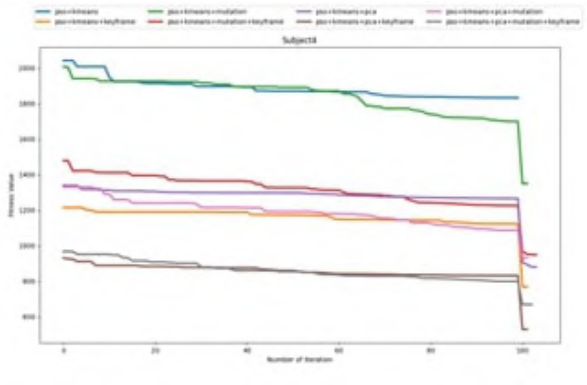

Fig. 52: The comparison of convergence in subject 8 of UTK.

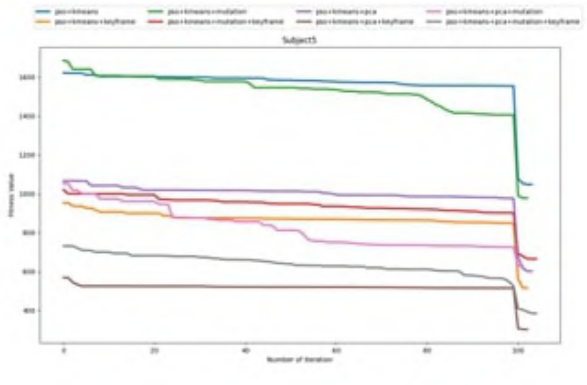

Fig. 53: The comparison of convergence in subject 9 of UTK.

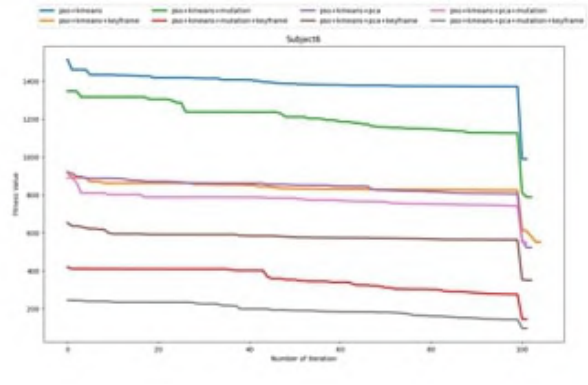

Fig. 54: The comparison of convergence in subject 10 of UTK.

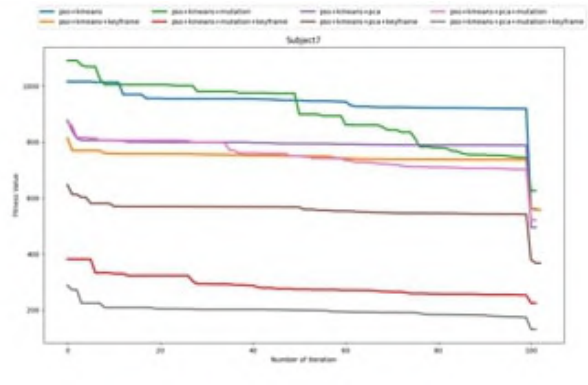

Fig. 55: The comparison of convergence in subject 1 of F3D.

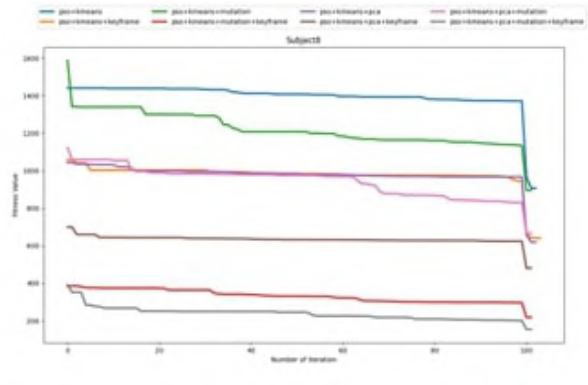

Fig. 56: The comparison of convergence in subject 2 of F3D.

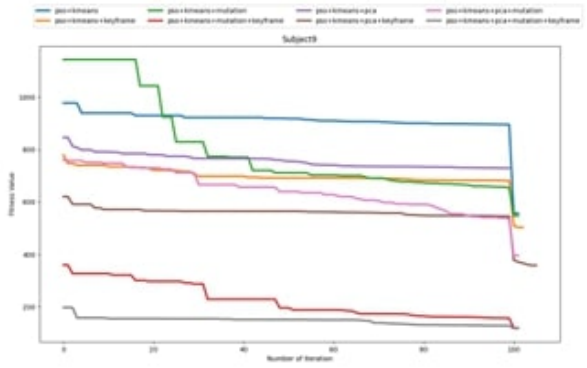

Fig. 57: The comparison of convergence in subject 3 of F3D.

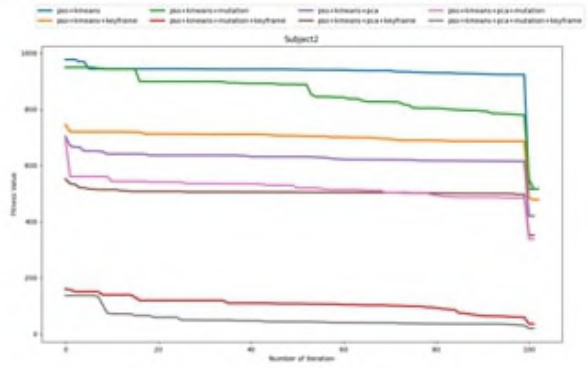

Fig. 60: The comparison of convergence in subject 6 of F3D.

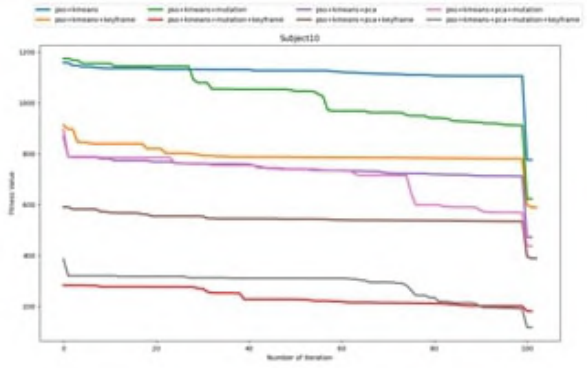

Fig. 58: The comparison of convergence in subject 4 of F3D.

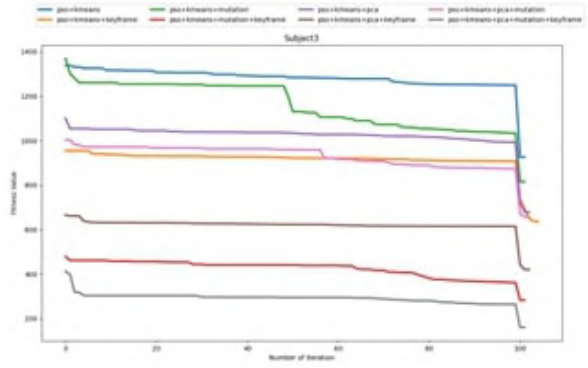

Fig. 61: The comparison of convergence in subject 7 of F3D.

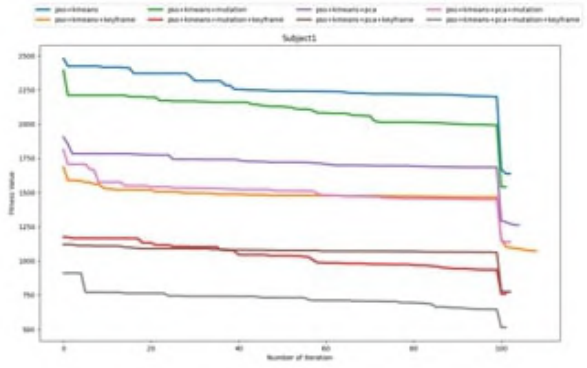

Fig. 59: The comparison of convergence in subject 5 of F3D.

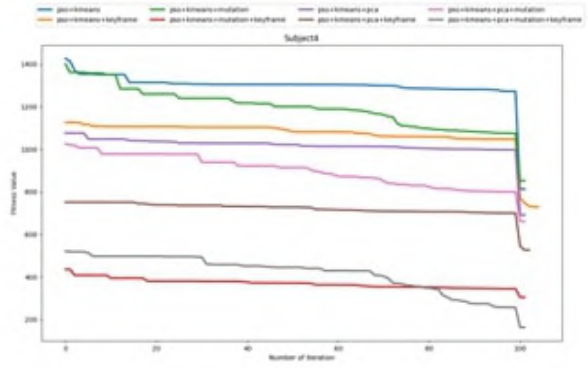

Fig. 62: The comparison of convergence in subject 8 of F3D.

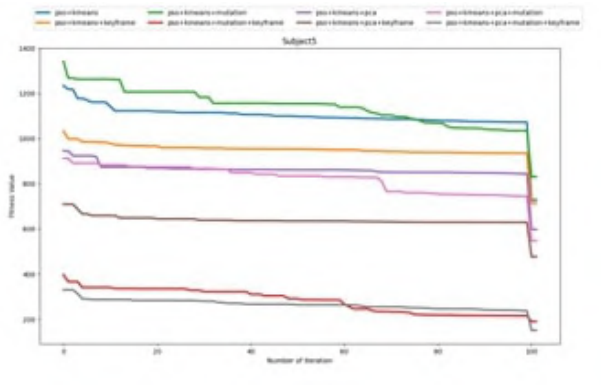

Fig. 63: The comparison of convergence in subject 9 of F3D.

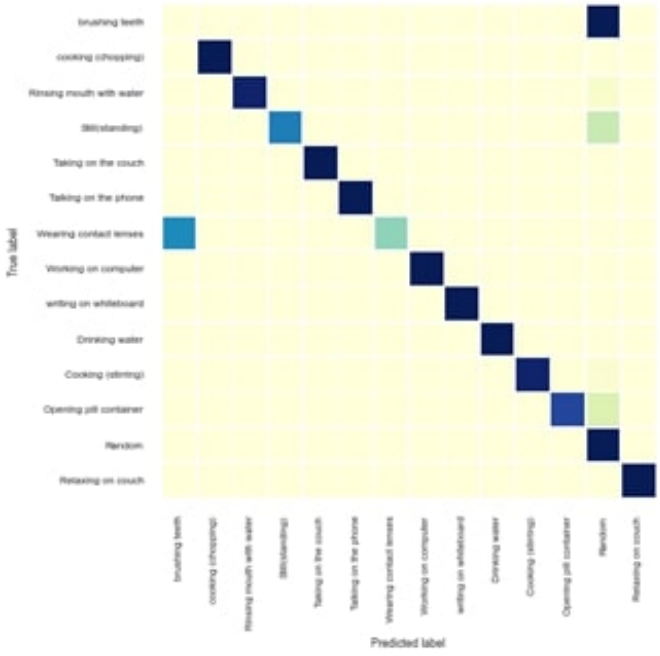

Fig. 64: The comparison of convergence in subject 10 of F3D.

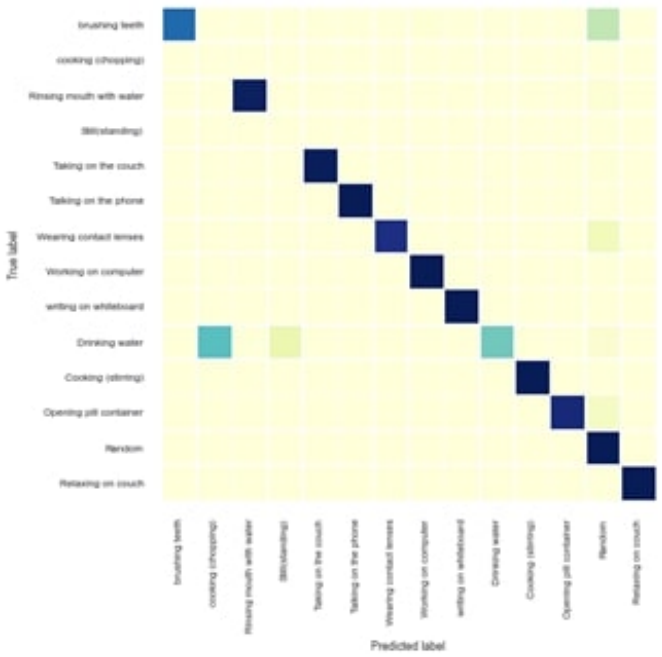

Fig. 65: The confusion matrix of HPGMK on the subject 1 of CAD-60.

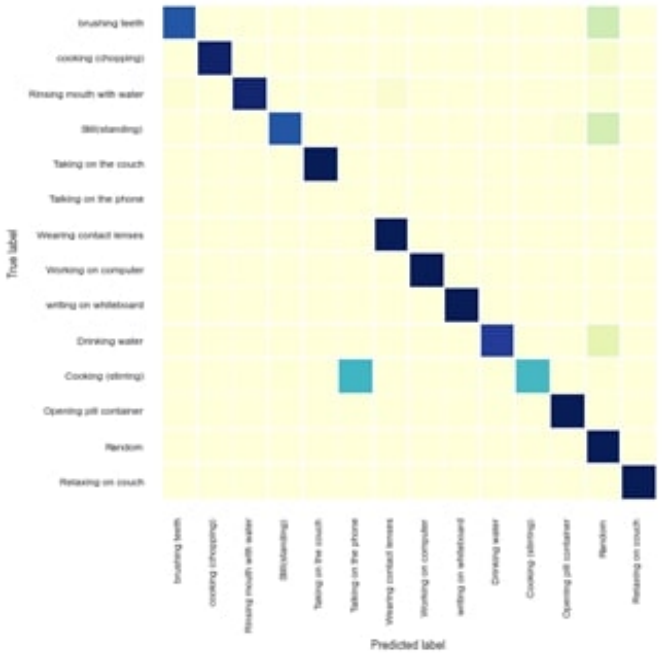

Fig. 66: The confusion matrix of HPGMK on the subject 2 of CAD-60.

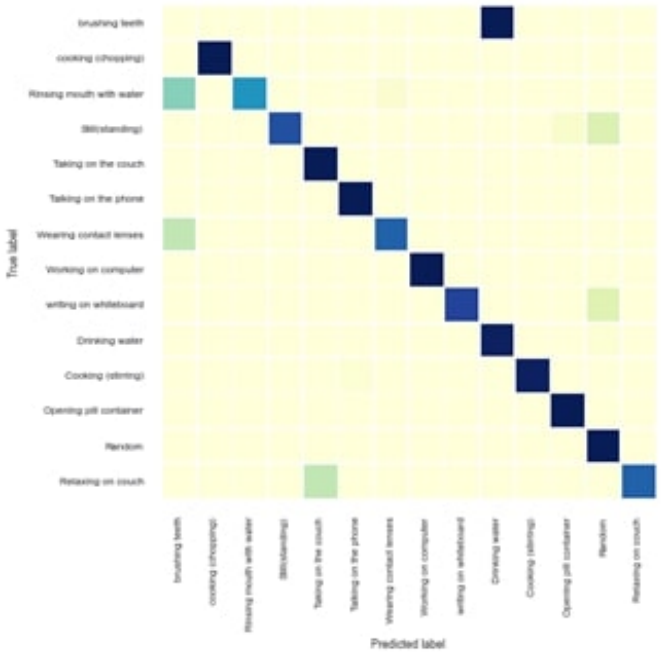

Fig. 67: The confusion matrix of HPGMK on the subject 3 of CAD-60.

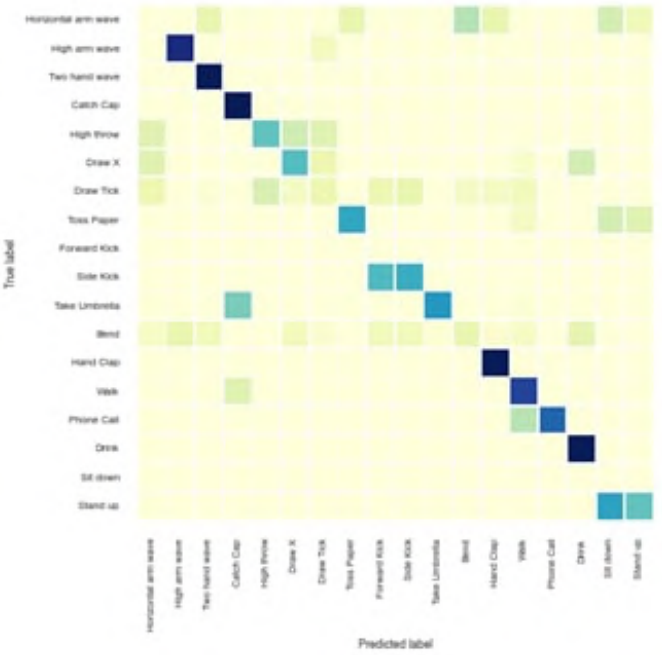

Fig. 69: The confusion matrix of HPGMK on the subject 1 of KARD.

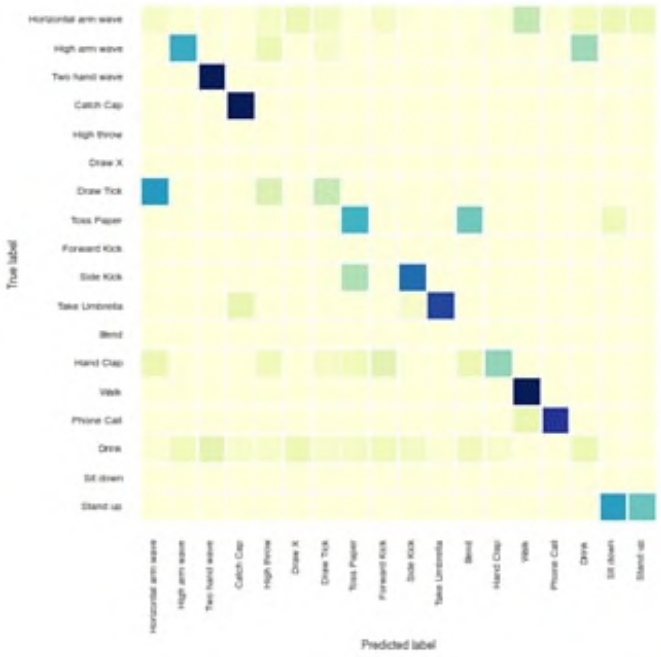

Fig. 68: The confusion matrix of HPGMK on the subject 4 of CAD-60.

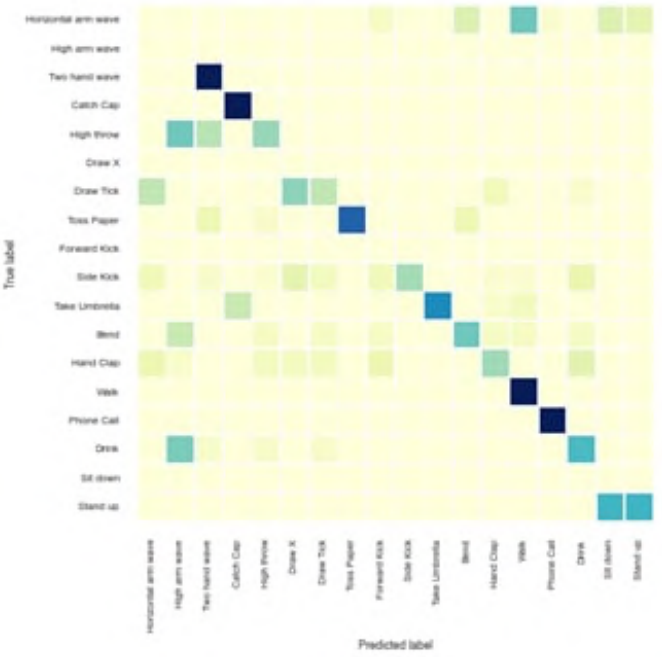

Fig. 70: The confusion matrix of HPGMK on the subject 2 of KARD.

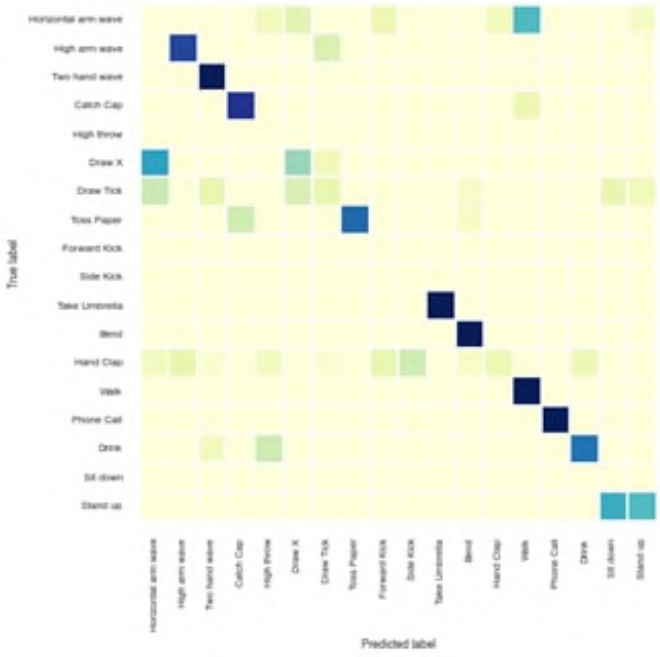

Fig. 71: The confusion matrix of HPGMK on the subject 3 of KARD.

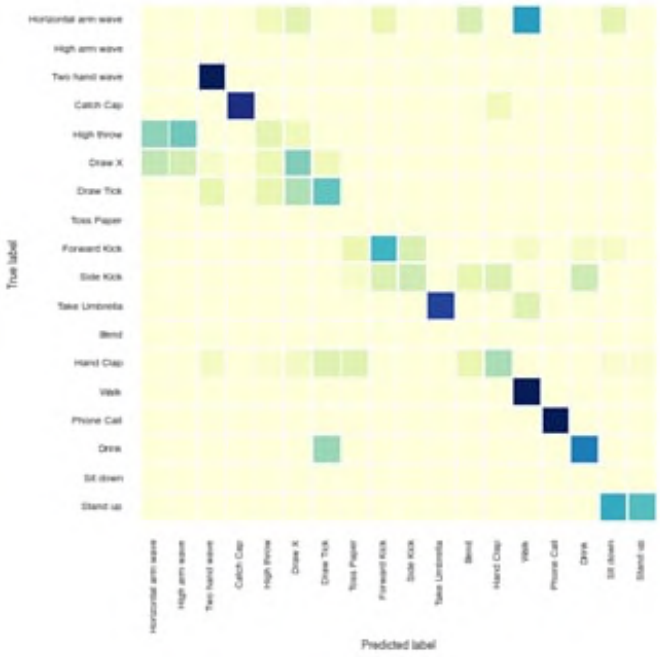

Fig. 72: The confusion matrix of HPGMK on the subject 4 of KARD.

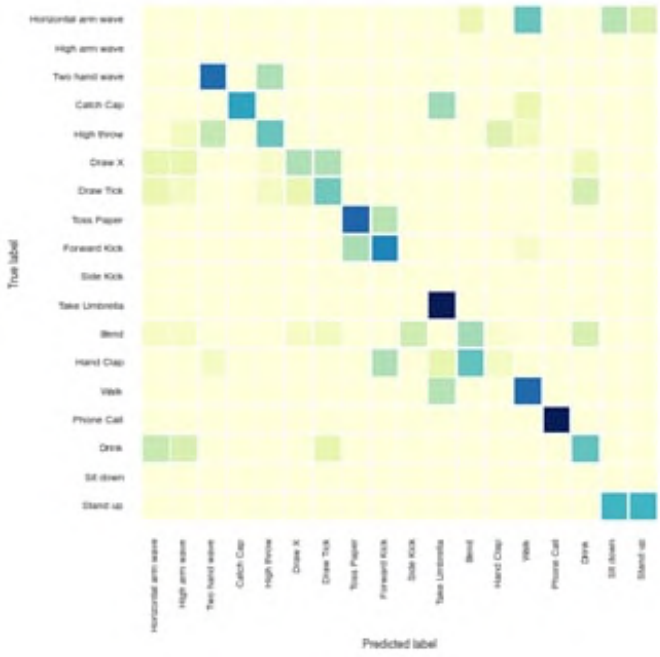

Fig. 73: The confusion matrix of HPGMK on the subject 5 of KARD.

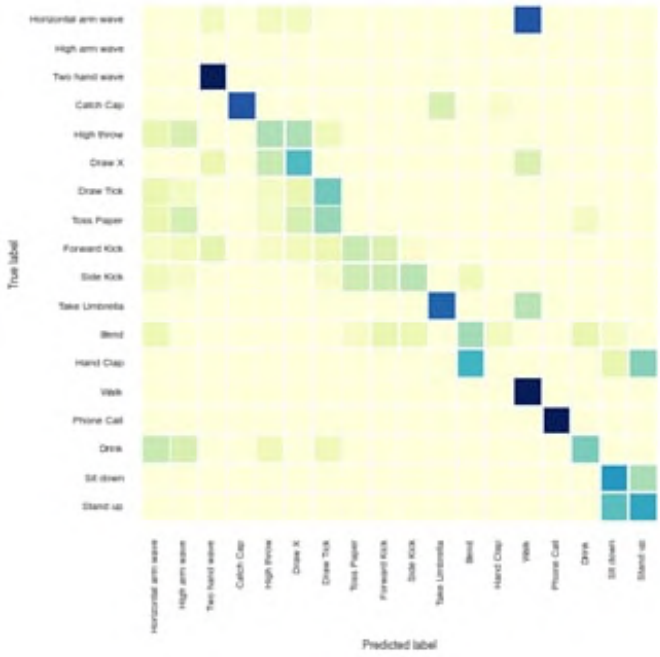

Fig. 74: The confusion matrix of HPGMK on the subject 6 of KARD.

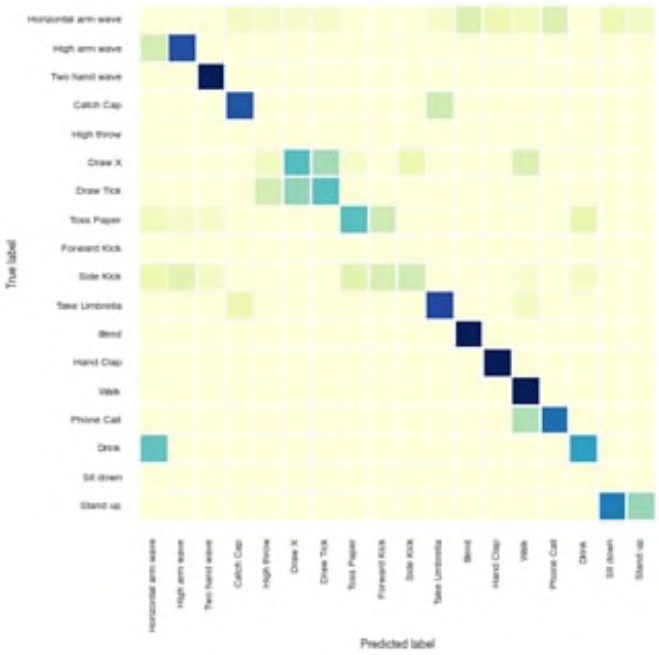

Fig. 75: The confusion matrix of HPGMK on the subject 7 of KARD.

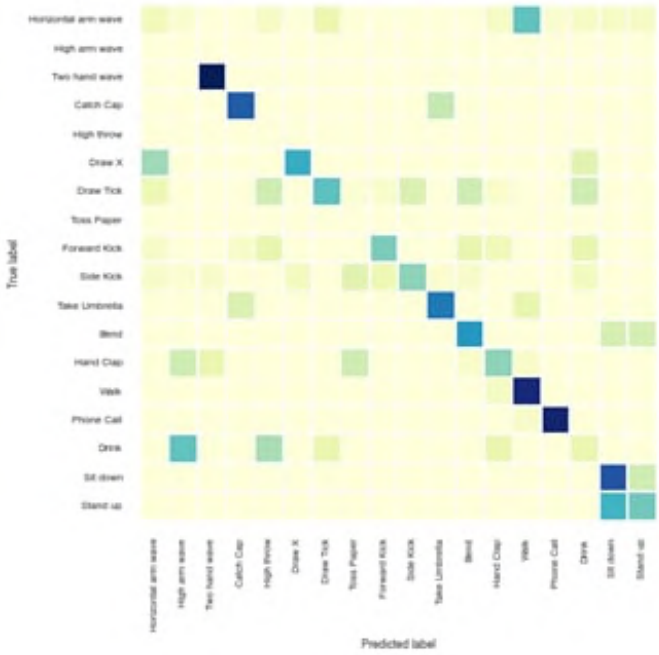

Fig. 77: The confusion matrix of HPGMK on the subject 9 of KARD.

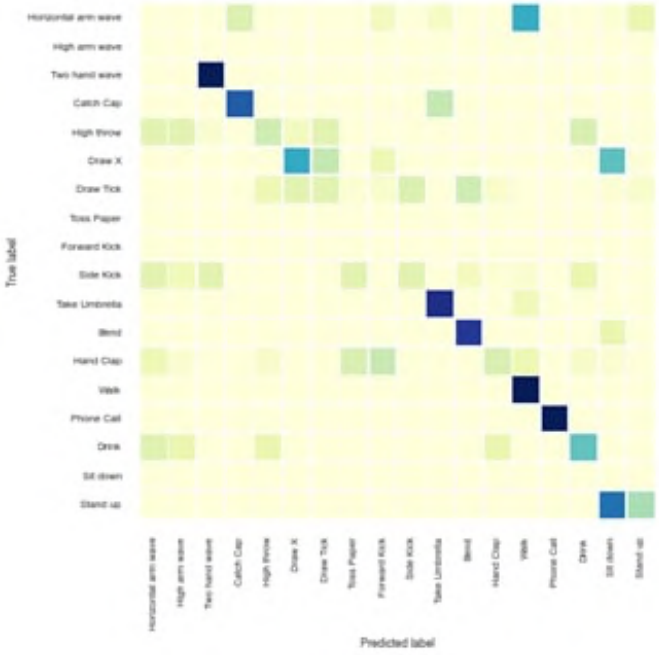

Fig. 76: The confusion matrix of HPGMK on the subject 8 of KARD.

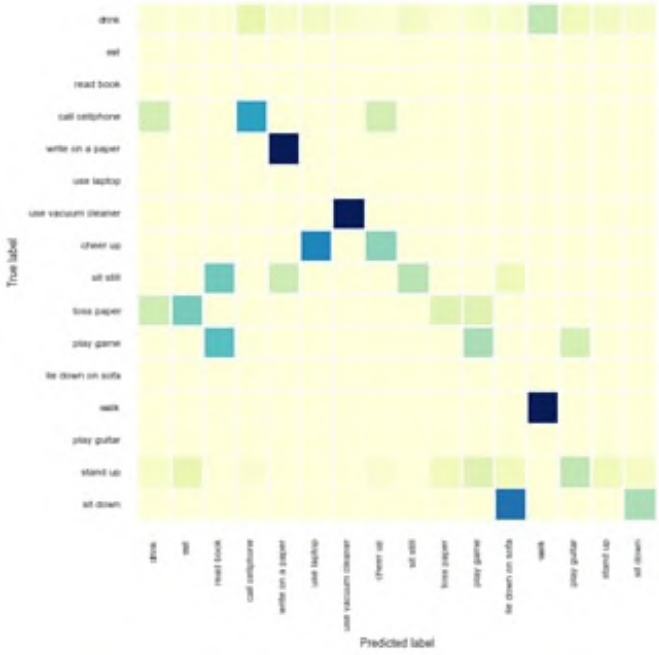

Fig. 78: The confusion matrix of HPGMK on the subject 10 of KARD.

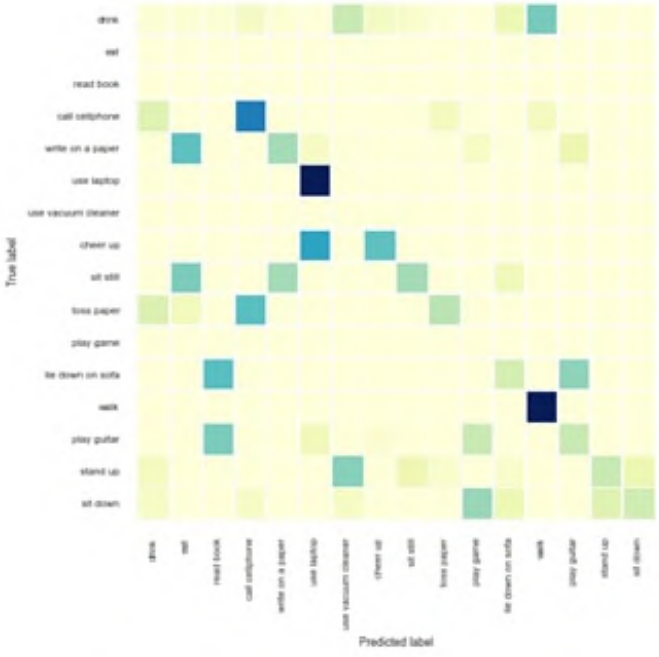

Fig. 79: The confusion matrix of HPGMK on the subject 1 of MSR.

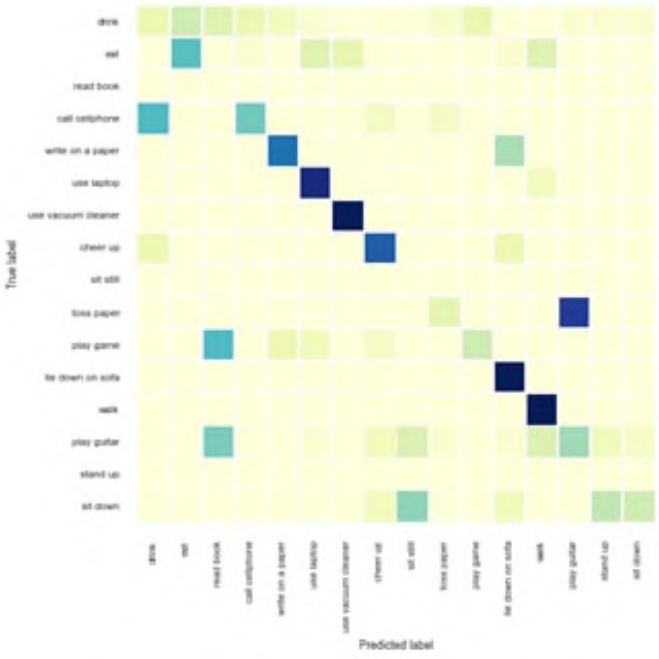

Fig. 80: The confusion matrix of HPGMK on the subject 2 of MSR.

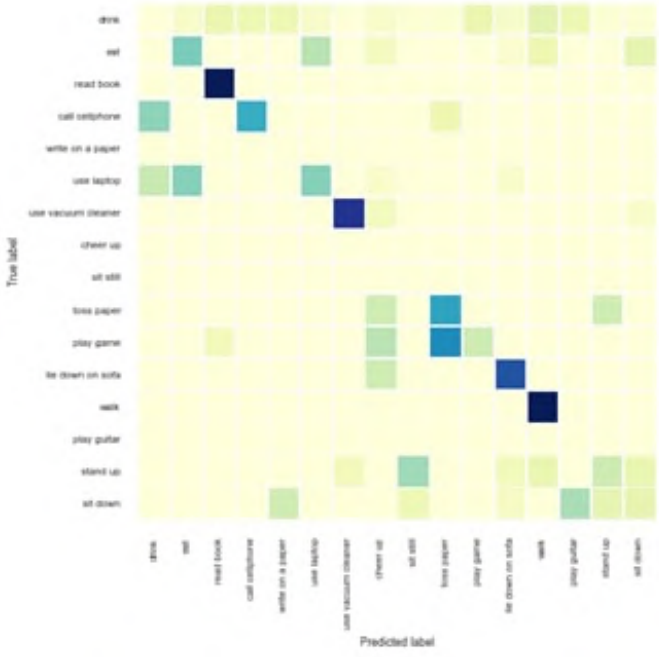

Fig. 81: The confusion matrix of HPGMK on the subject 3 of MSR.

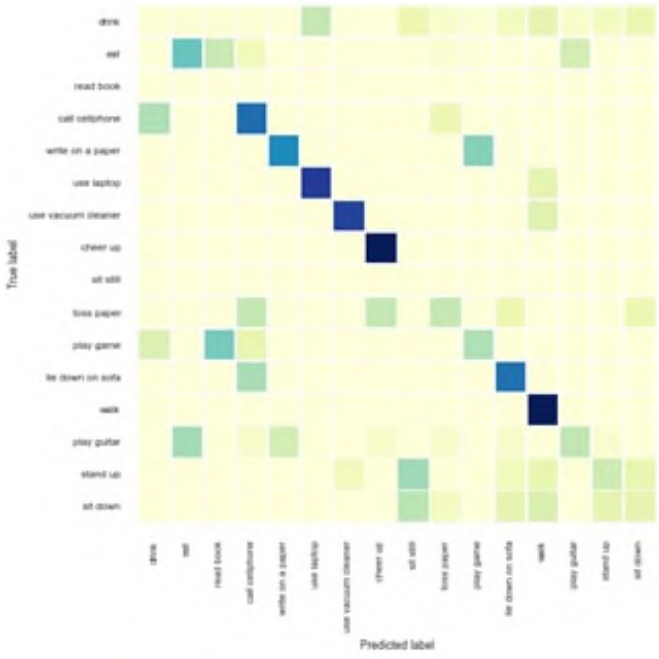

Fig. 82: The confusion matrix of HPGMK on the subject 4 of MSR.

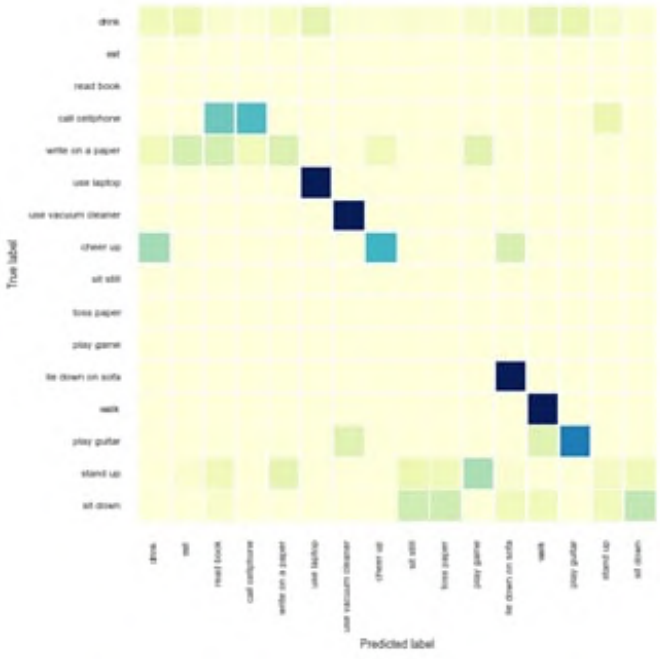

Fig. 83: The confusion matrix of HPGMK on the subject 5 of MSR.

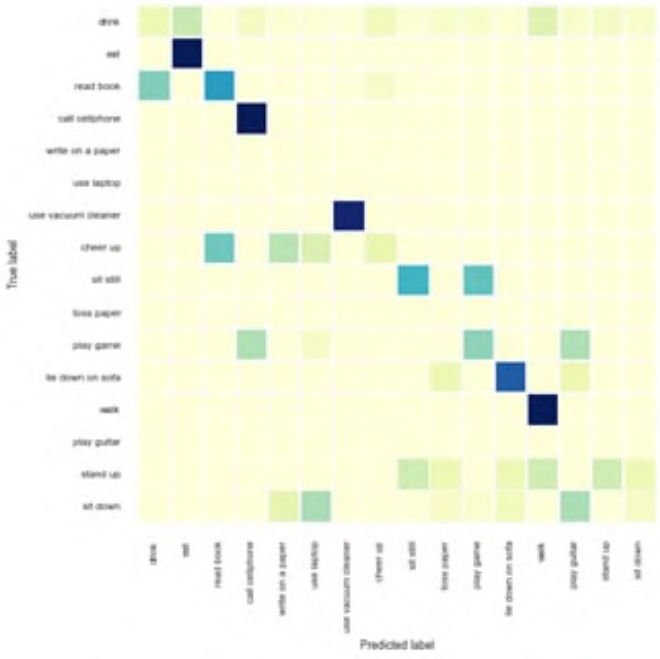

Fig. 84: The confusion matrix of HPGMK on the subject 6 of MSR.

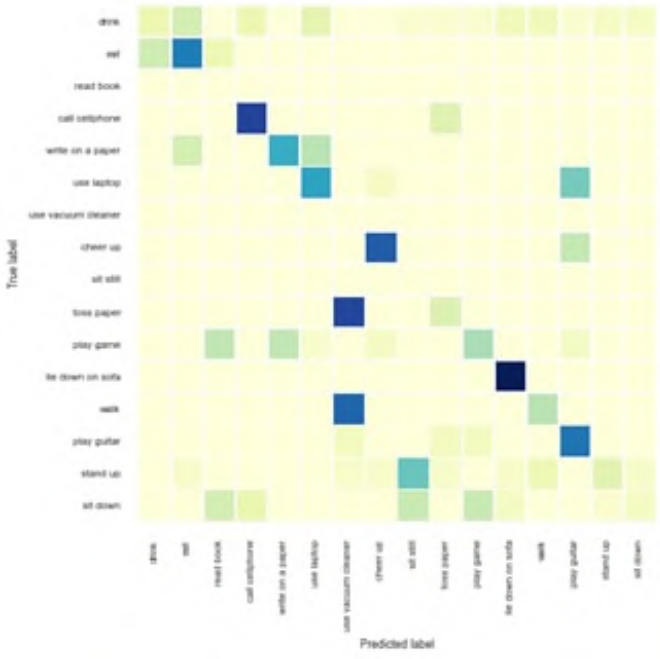

Fig. 85: The confusion matrix of HPGMK on the subject 7 of MSR.

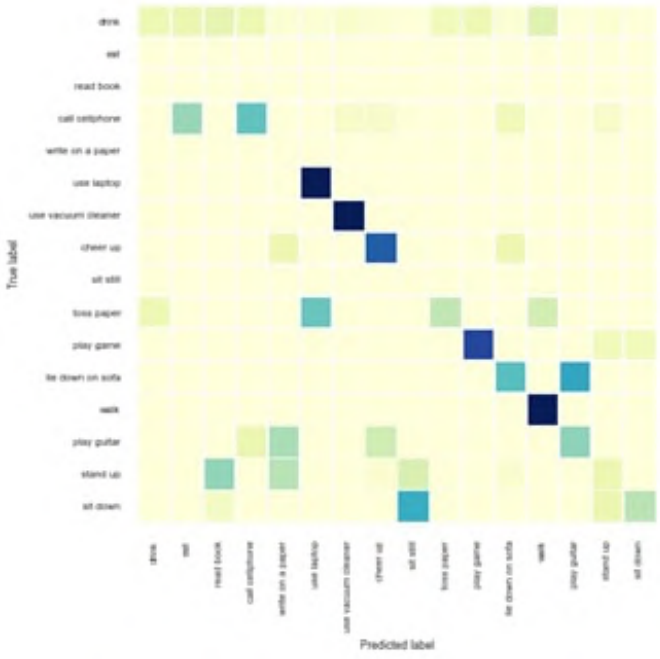

Fig. 86: The confusion matrix of HPGMK on the subject 8 of MSR.

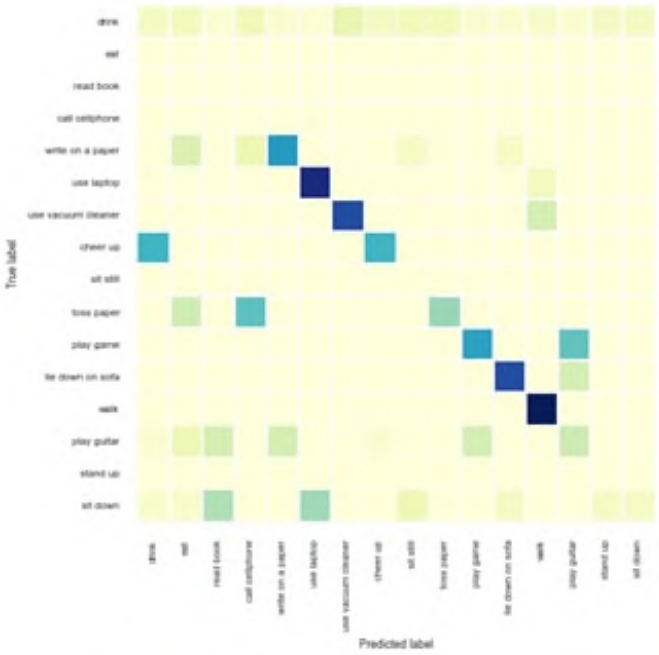

Fig. 87: The confusion matrix of HPGMK on the subject 9 of MSR.

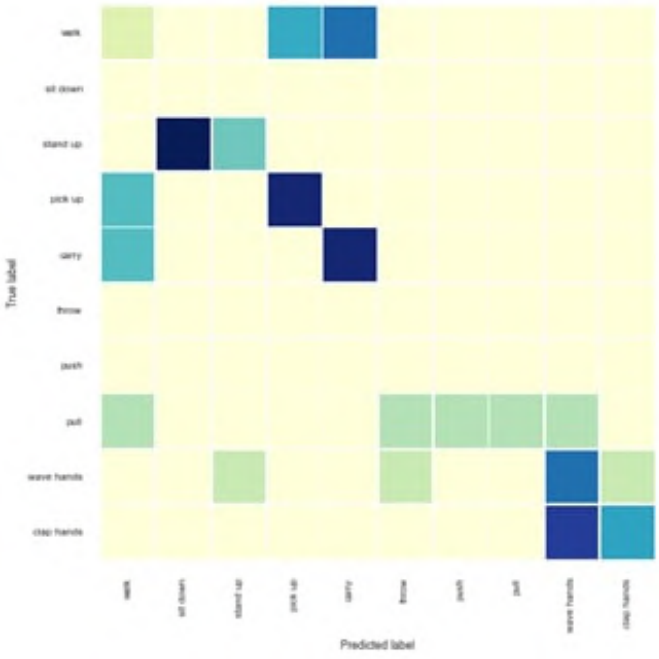

Fig. 88: The confusion matrix of HPGMK on the subject 10 of MSR.

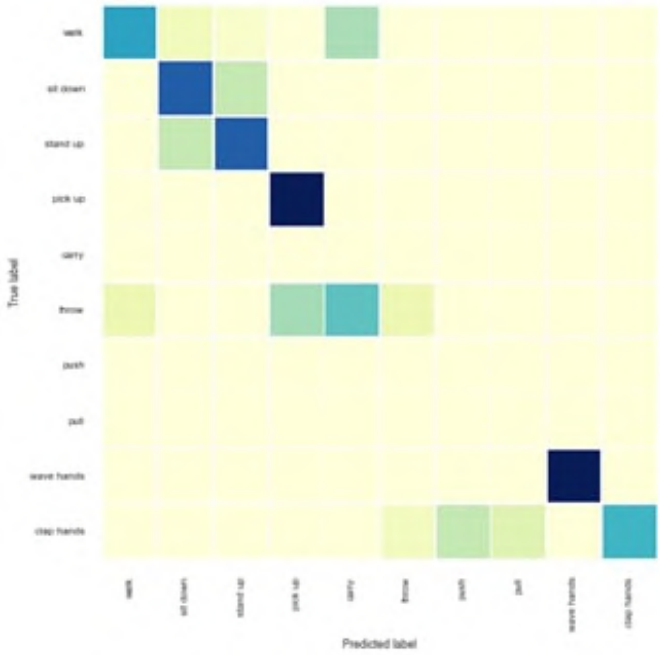

Fig. 89: The confusion matrix of HPGMK on the subject 1 of UTK.

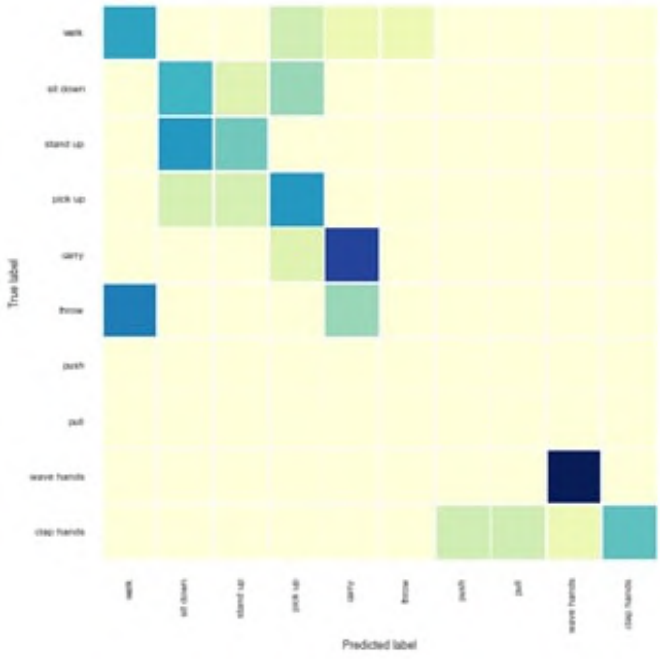

Fig. 90: The confusion matrix of HPGMK on the subject 2 of UTK.

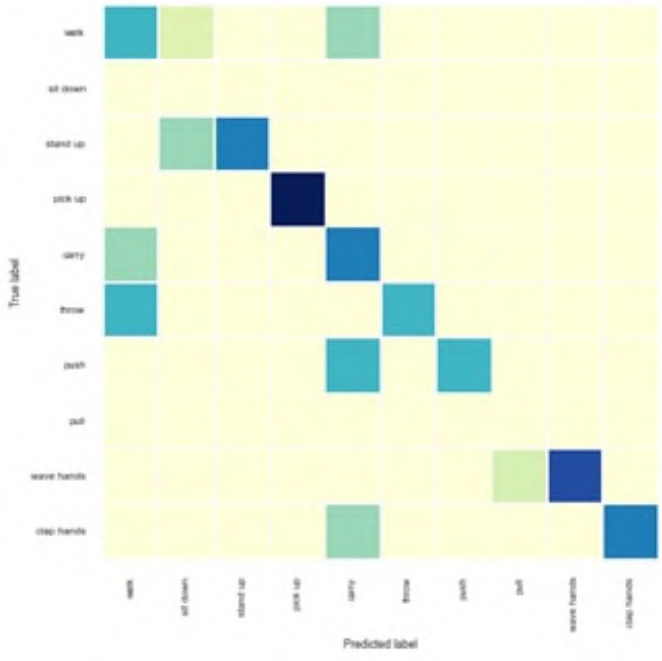

Fig. 91: The confusion matrix of HPGMK on the subject 3 of UTK.

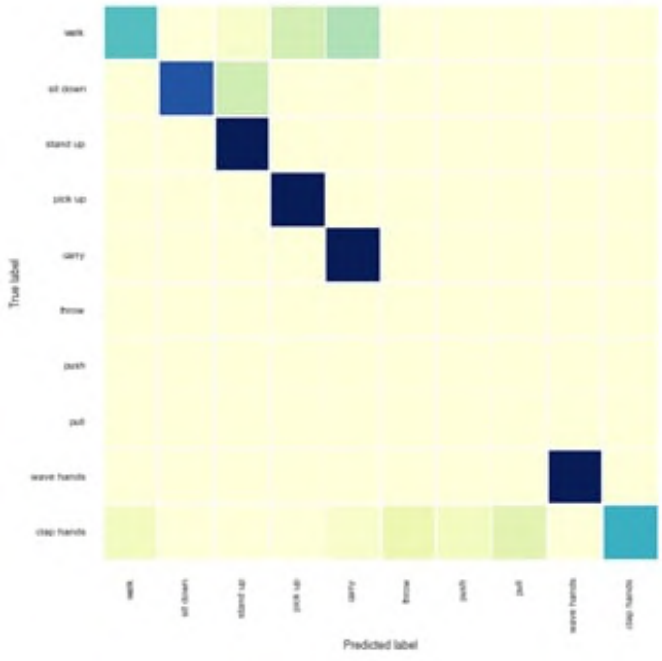

Fig. 92: The confusion matrix of HPGMK on the subject 4 of UTK.

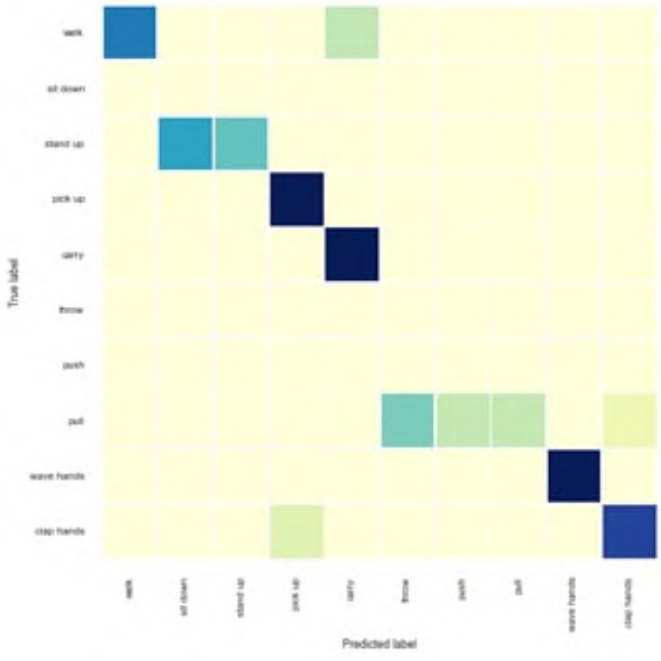

Fig. 93: The confusion matrix of HPGMK on the subject 5 of UTK.

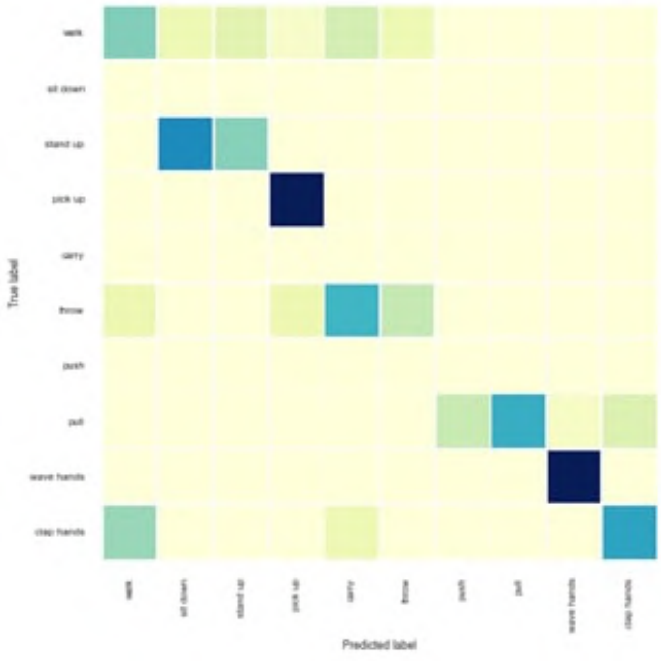

Fig. 94: The confusion matrix of HPGMK on the subject 6 of UTK.

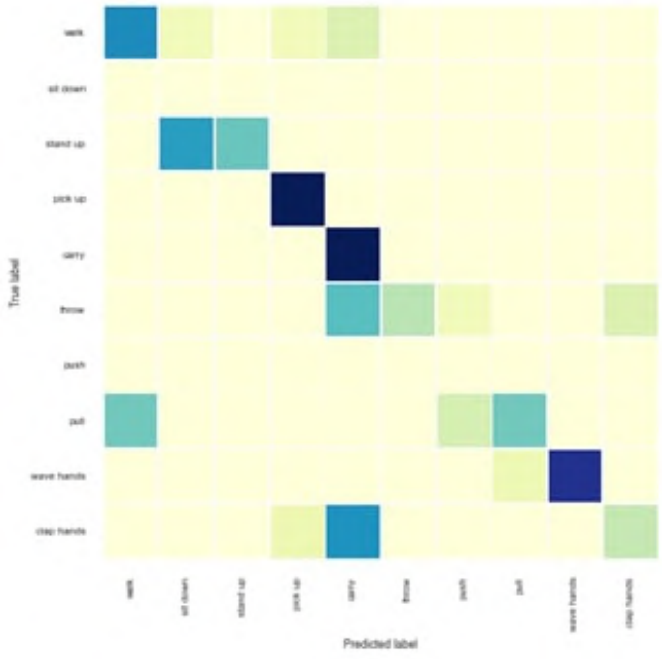

Fig. 95: The confusion matrix of HPGMK on the subject 7 of UTK.

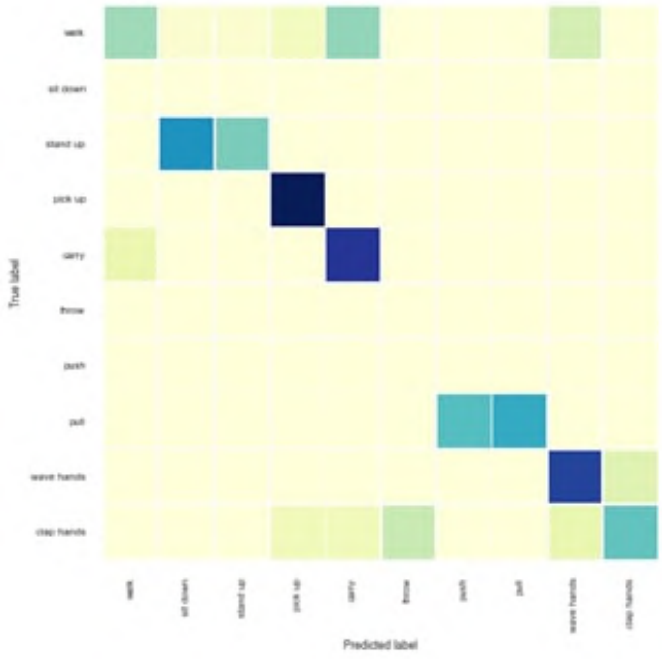

Fig. 96: The confusion matrix of HPGMK on the subject 8 of UTK.

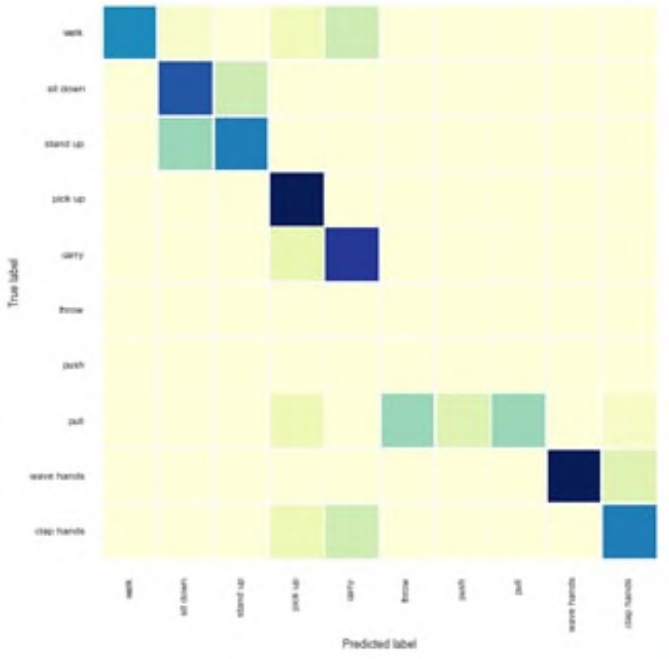

Fig. 97: The confusion matrix of HPGMK on the subject 9 of UTK.

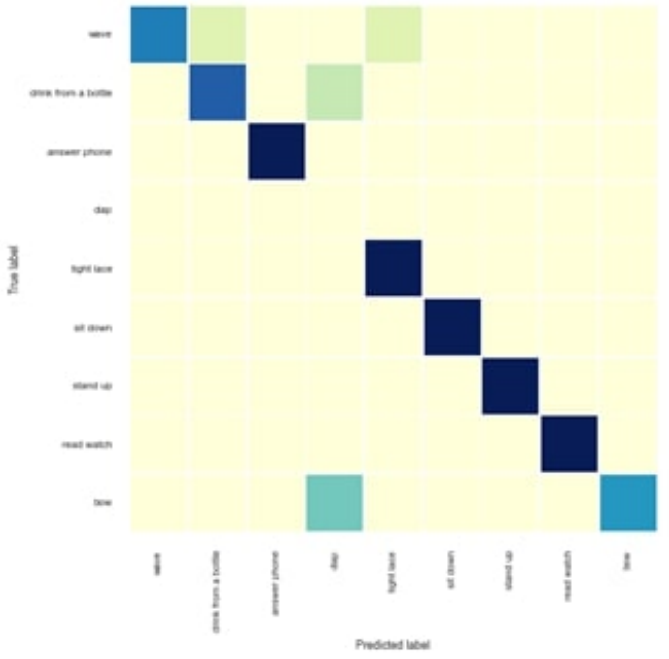

Fig. 98: The confusion matrix of HPGMK on the subject 10 of UTK.

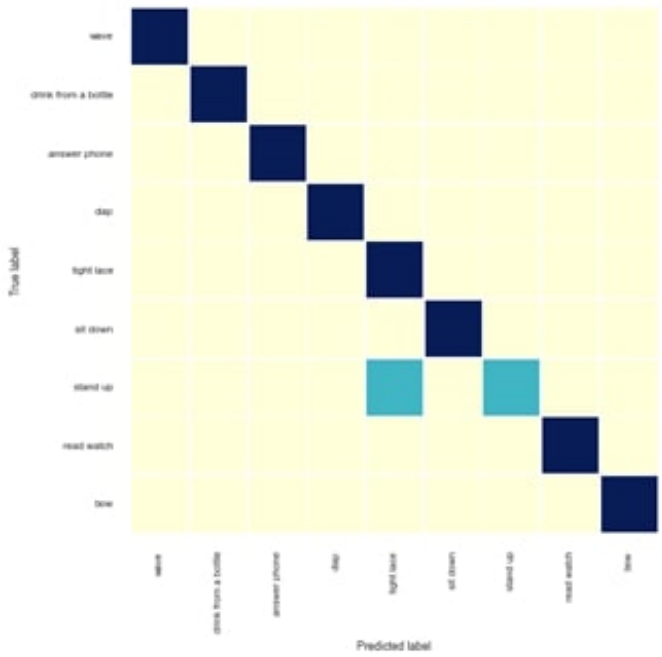

Fig. 99: The confusion matrix of HPGMK on the subject 1 of F3D.

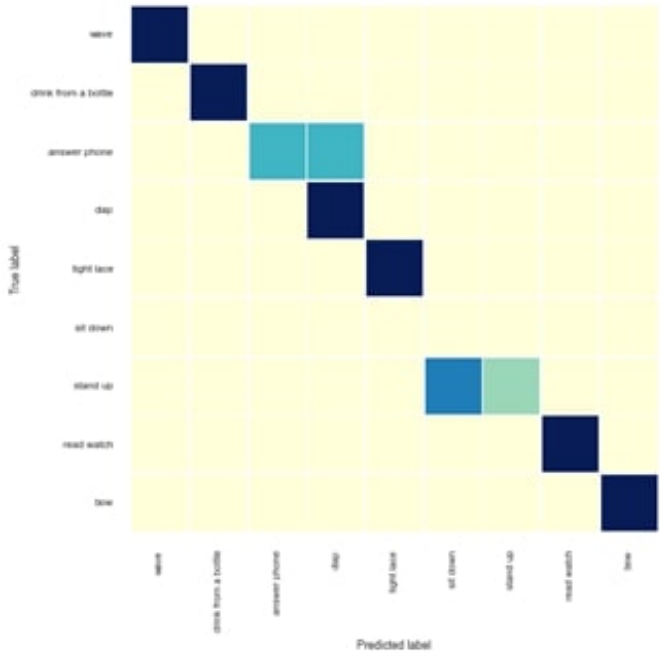

Fig. 100: The confusion matrix of HPGMK on the subject 2 of F3D.

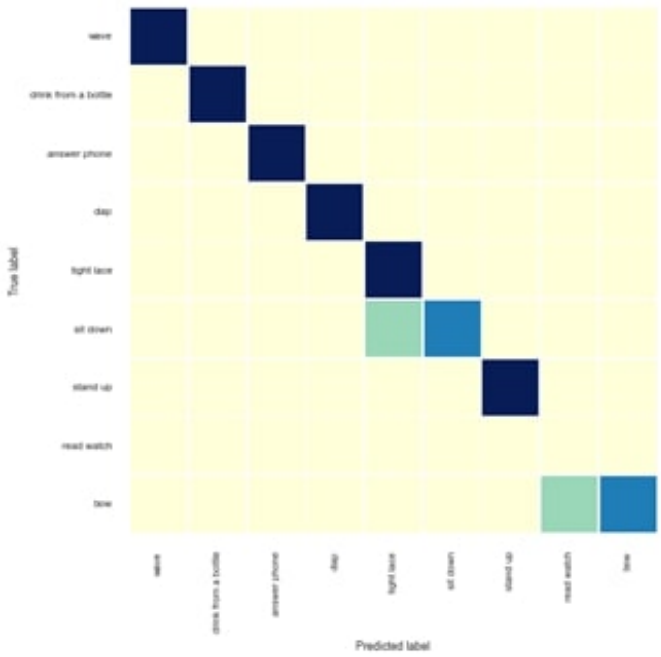

Fig. 101: The confusion matrix of HPGMK on the subject 3 of F3D.

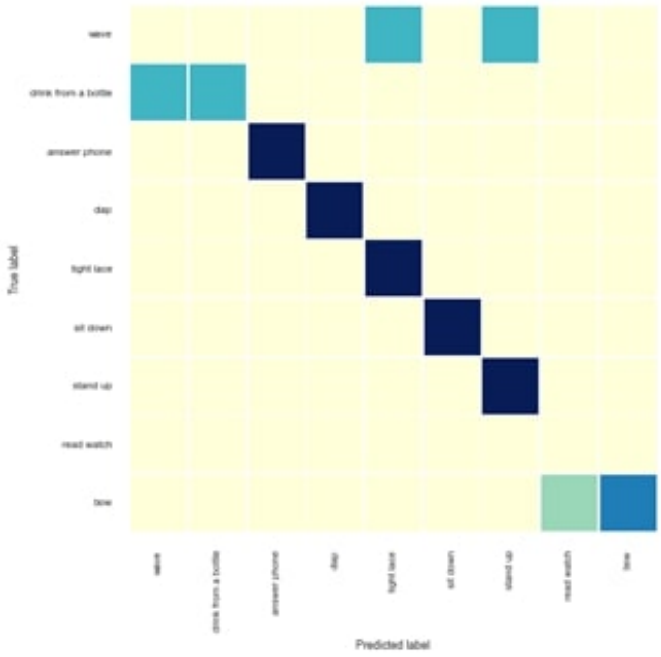

Fig. 102: The confusion matrix of HPGMK on the subject 4 of F3D.

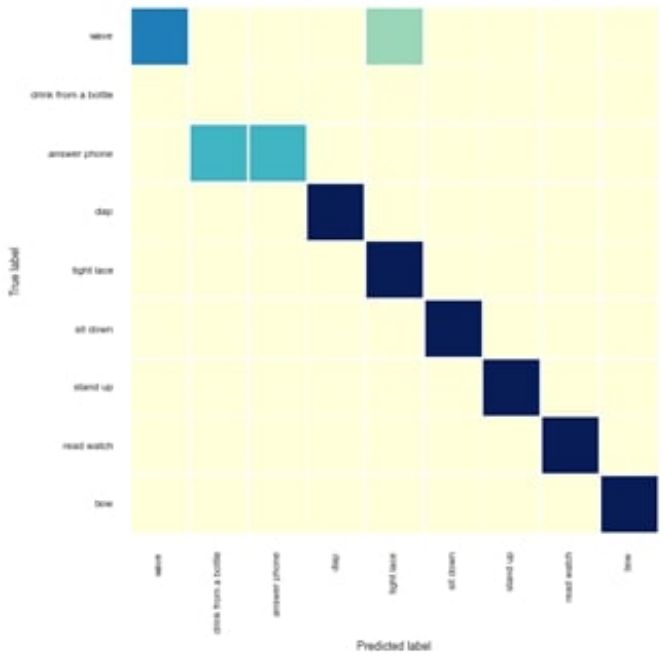

Fig. 103: The confusion matrix of HPGMK on the subject 5 of F3D.

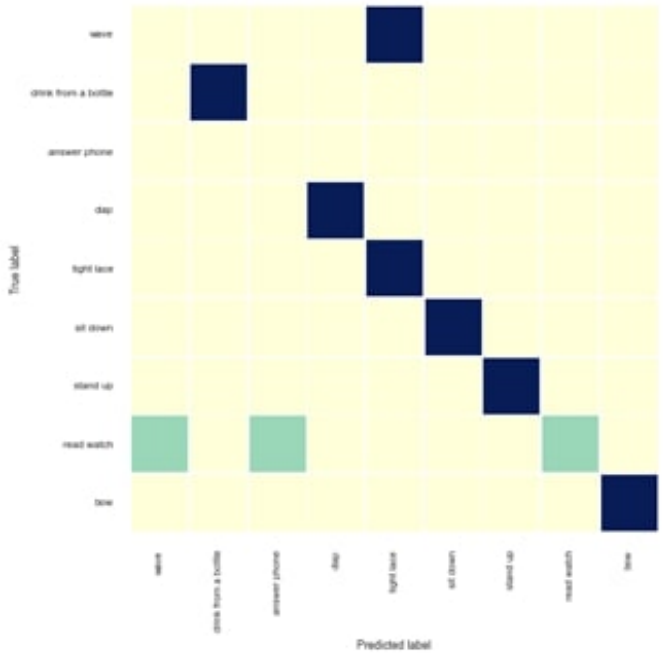

Fig. 104: The confusion matrix of HPGMK on the subject 6 of F3D.

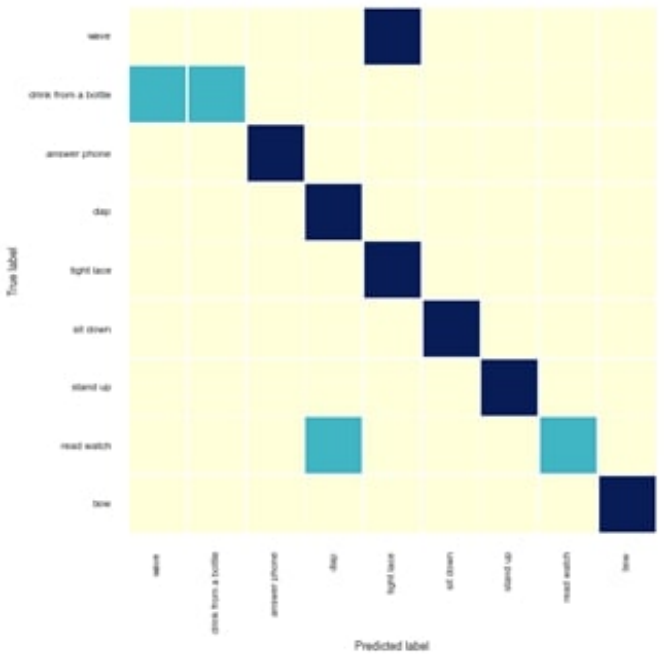

Fig. 105: The confusion matrix of HPGMK on the subject 7 of F3D.

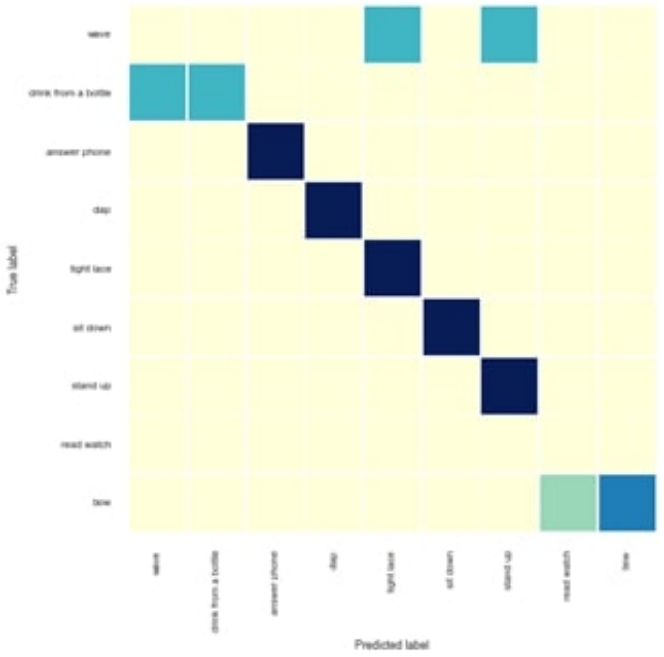

Fig. 106: The confusion matrix of HPGMK on the subject 8 of F3D.

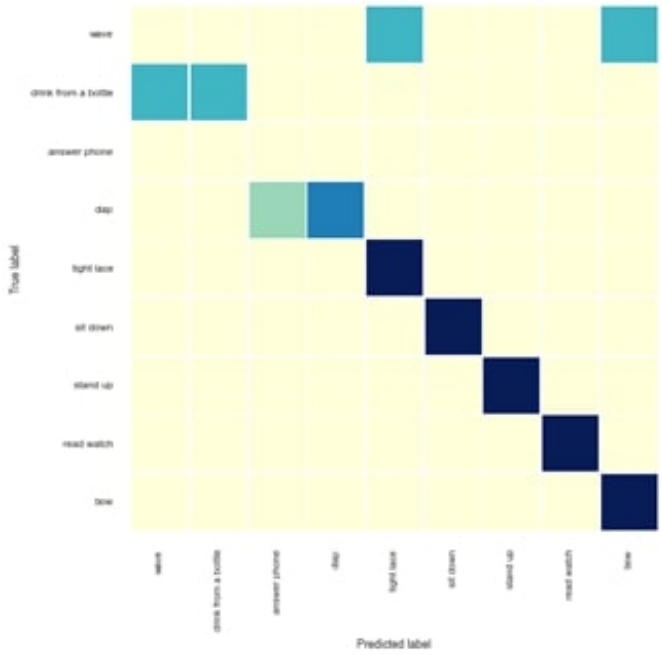

Fig. 107: The confusion matrix of HPGMK on the subject 9 of F3D.

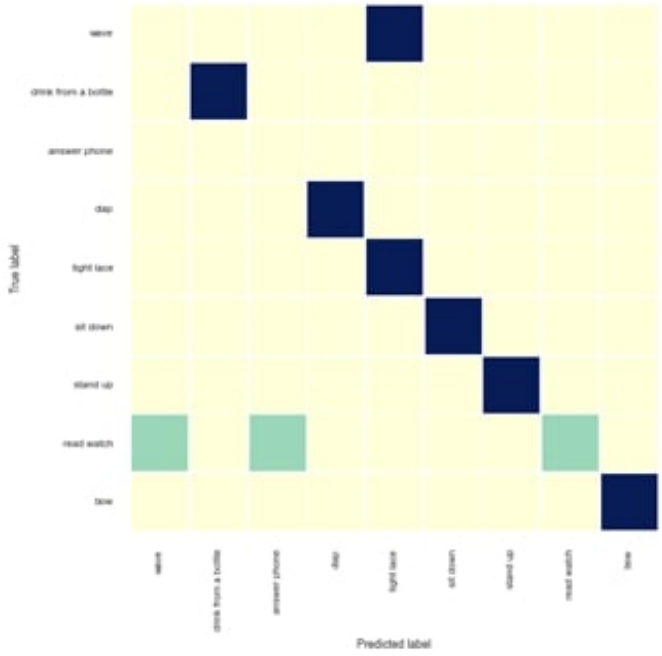

Fig. 108: The confusion matrix of HPGMK on the subject 10 of F3D.